Published in final edited form as:
J Comp Neurol. 2014 February ; 522(2): . doi:10.1002/cne.23405.

Splicing factor TRA2B is required for neural progenitor survival

Jacqueline M Roberts[1], **Hanane Ennajdaoui**[1], **Carina Edmondson**[1], **Brunhilde Wirth**[2], **Jeremy Sanford**[1], and **Bin Chen**[1,*]

[1]Department of Molecular, Cell, and Developmental Biology, University of California, Santa Cruz, CA 95064, USA

[2]Institute of Human Genetics, Institute for Genetics and Center for Molecular Medicine Cologne, University of Cologne, Cologne 50931, Germany

Abstract

Alternative splicing of pre-mRNAs can rapidly regulate the expression of large groups of proteins. The RNA binding protein TRA2B (SFRS10) plays well-established roles in developmentally regulated alternative splicing during *Drosophila* sexual differentiation. TRA2B is also essential for mammalian embryogenesis and is implicated in numerous human diseases. Precise regulation of alternative splicing is critical to the development and function of the central nervous system; however the requirements for specific splicing factors in neurogenesis are poorly understood. In this study we focus on the role of TRA2B in mammalian brain development. We show that, during murine cortical neurogenesis, TRA2B is expressed in both neural progenitors and cortical projection neurons. Using cortex-specific *Tra2b* mutant mice, we find that TRA2B depletion results in apoptosis of the neural progenitor cells as well as disorganization of the cortical plate. Thus, TRA2B is essential for proper development of the cerebral cortex.

Keywords

TRA2B; cerebral cortex; development; splicing; neural progenitor; SR protein

Introduction

The cerebral cortex is the seat for the highest level sensory, motor, and cognitive functions; and a diverse collection of cell types is required to achieve its complex functions. This six-layered structure is composed of projection neurons, interneurons, and glia. Projection neurons inhabiting the same cortical layer tend to share similar axonal targets, morphology, and gene expression profiles (DeFelipe, 1993; Caviness and Takahashi, 1995; Migliore and Shepherd, 2005; Molyneaux et al., 2007; Kwan et al., 2012). During cerebral cortex development, progenitor cells in the ventricular zone sequentially generate different types of cortical projection neurons. The earliest born neurons form the preplate, which is subsequently split into the marginal zone and the subplate by incoming cortical plate neurons. Neurons in the cortical plate are generated in an inside-out pattern; the early born cortical neurons form layer 6, followed by neurons of layer 5, then layer 4. Neurons of layer 3 and 2 are generated last (Angevine and Sidman, 1961; Berry and Rogers, 1965).

[*] Corresponding Author: Bin Chen Department of Molecular, Cell, and Developmental Biology University of California 1156 High St. Santa Cruz, CA 95064 Phone: 831-459-2630 FAX: 831-459-3139 bchen@ucsc.edu.

Conflict of interest statement
The authors declare no conflict of interest in the present study.

The process of generating mature neurons from proliferating neural progenitors is tightly regulated. Many studies to date have uncovered the critical functions of canonical signaling pathways (Rallu et al., 2002; Götz and Huttner, 2005; Hansen et al., 2010), transcription factors (Leone et al., 2008; Hoch et al., 2009), and miRNAs (Volvert et al., 2012) in controlling neuronal development. Alternative pre-mRNA splicing is another powerful way to regulate gene function, and the vast majority of mammalian pre-mRNA transcripts undergo alternative splicing (Castle et al., 2008; Wang et al., 2008). Alternative mRNA isoforms are presumed to be translated into proteins with different sequences and functions, and as many as 30% of alternative splicing events generate unstable mRNA isoforms that are destroyed through nonsense mediated decay (Lewis et al., 2003; Ni et al., 2007). RNA binding proteins are major regulators of alternative splicing and are important in diverse developmental and disease pathways (Boutz et al., 2007; Zheng et al., 2012; Eom et al., 2013). The strong evolutionary conservation of brain-specific alternative splicing events underscores the biological importance of this process to brain development and function (Barbosa-Morais et al., 2012; Merkin et al., 2012). However, researchers have only begun to demonstrate the functions of splicing factors in generating the complex neuronal specific transcriptome (Li et al., 2007; Calarco et al., 2011; Raj et al., 2011).

The serine and arginine-rich protein (SR protein) family of RNA binding proteins are essential, evolutionarily conserved, pre-mRNA splicing factors (Wang et al., 1996; Busch and Hertel, 2012; Califice et al., 2012). SR proteins are involved in both constitutive and alternative splicing processes, as well as other modes of RNA metabolism (Sanford et al., 2005; Zhong et al., 2009). They are generally composed of one or more RNA recognition motifs, through which they recognize exonic splice enhancers (ESEs) at an early stage in spliceosome assembly (Kohtz et al., 1994; Staknis and Reed, 1994; Graveley and Maniatis, 1998). SR proteins also contain a carboxyl-terminal serine-arginine rich domain (RS domain) known to be involved in both protein-protein and protein-RNA interactions (Wu and Maniatis, 1993; Shen and Green, 2004). These interactions are important for selecting splice sites and establishing exon identity (Black, 2003; Long and Caceres, 2009). Although SR proteins share structural and functional similarities, different SR protein family members have distinct, non-redundant functions in specific tissues or development processes (Zahler et al., 1993; Wang and Manley, 1995; Mende et al., 2010).

We identified the RS domain-containing splicing factor, TRA2B, as a candidate for regulating the development of the cerebral cortex. TRA2B is structurally and functionally related to the classical SR proteins, and functions in developmentally regulated alternative splicing pathways (Elliott et al., 2012). The TRA2B homologue, Tra2, was initially implicated with other splicing factors in regulating development of sex-specific morphology and behavior in *Drosophila* (Amrein et al., 1988; Taylor et al., 1994; Lopez, 1998). Mammalian TRA2B has been shown to influence alternative splicing of transcripts necessary for the proper functions of multiple tissues including smooth muscle, testis, and neurons (Daoud et al., 1999; Li et al., 2007; Grellscheid et al., 2011). Decreased levels of TRA2B have been observed in human diseases including stroke, breast cancer, and neurodegeneration (Watermann et al., 2006; Li et al., 2007). Important examples of crucial splicing events regulated by TRA2B are *Tau* exon 10 inclusion and *SMN1* and *SMN2* exon 7 inclusion (Hofmann et al., 2000; Hofmann and Wirth, 2002; Wang et al., 2005). Mis-regulation of *Tau* pre-mRNA splicing results in abnormal protein aggregation, which is a common feature in many neurodegenerative diseases (Hutton et al., 1998; D'Souza et al., 1999; Jellinger, 2012). TRA2B influences *Tau* isoform expression by directly binding *Tau* exon 10 and regulating its inclusion (Wang et al., 2005). Overexpression of this *Tau* mRNA isoform has been identified as the cause of Frontotemporal Dementia with Parkinsonism linked to chromosome 17 (FTDP-17), and has been linked to Alzheimer's and dementia syndromes (Caffrey and Wade-Martins, 2007; Dawson et al., 2007). A mutation in *SMN1* is

the cause of spinal muscular atrophy (SMA), which is characterized by degeneration of spinal motor neurons. Disease severity is reduced by increased functional SMN2 production through increased inclusion of *SMN2* exon 7. The overexpression of TRA2B increases correct *SMN2* splicing, and transfection of targeted oligonucleotides which enhance the recruitment of TRA2B efficiently increases SMN2 production (Hofmann et al., 2000; Owen et al., 2011). In SMA, the use of histone deacetylase inhibitors (HDACi) which upregulate TRA2B significantly increased SMN protein levels (Garbes et al., 2013; Wirth et al., 2013). These studies suggest that TRA2B-regulated splicing events may be novel therapeutic targets for treating neurodegeneration (Hartmann et al., 2001; Stoilov et al., 2004; Anderson et al., 2012).

Recent publications have shown that ubiquitous *Tra2b* knockout mice cannot survive past embryonic day 7.5 (E7.5) (Mende et al., 2010), indicating that TRA2B is an essential splicing factor in mammals. Unfortunately, the early lethality of the *Tra2b* mutant mice prevented an assessment of its function in brain development. Here we employ a conditional knock out approach to investigate the function of TRA2B during the development of the cerebral cortex. We have found that TRA2B is expressed in both progenitor cells and postmitotic neurons throughout cortical development. In the cortex-specific *Tra2b* knockout mice, extensive apoptosis of neural progenitor cells has been observed, resulting in cortices lacking most of the neocortical tissues at birth. In addition, differentiation of cortical layers and development of projection neuron axons are both defective. Our results demonstrate that TRA2B is critical for the survival of neural progenitor cells and proper differentiation of cortical projection neurons.

Materials and Methods

All the antibodies used in this study are listed in Table 1. The abbreviations used are listed in Table 2.

Animals

Experiments were carried out in accordance with protocols approved by the IACUC at University of California at Santa Cruz, and were performed in accordance with institutional and federal guidelines.

Generation and genotyping of *Tra2b-floxed* (Mende et al., 2010), *Emx1-IREScre* (Gorski et al., 2002), *RCE-GFP* (Miyoshi et al., 2010), and *Fezf2-PLAP* (Chen et al., 2005 a) mice have been previously published. For timed breeding, female and male mice were put together overnight, and the female mice were checked the next morning for the presence of a vaginal plug. The day of vaginal plug detection was designated as embryonic day 0.5 (E0.5). The day of birth was designated as postnatal day 0 (P0).

Immunohistochemistry

Postnatal mice were perfused with phosphate buffered saline, pH 7.4 (1x PBS), followed by 4% paraformaldehyde (PFA) before dissection. Brains of both postnatal and embryonic mice were fixed overnight in 4% PFA at 4°C, immersed overnight in 30% sucrose at 4°C, embedded in Tissue-tek O.C.T. (Sakura Finetek USA, Torrance, CA), and stored at −80°C. The frozen tissue was sliced into 20μm sections onto Superfrost Plus Slides (Fisher Scientific, Pittsburgh, PA). Slides were allowed to dry at room temperature for 20 minutes before being placed in blocking buffer (5% horse serum, 0.5% Triton x-100, 1x PBS) for 30 minutes. Sections were then incubated overnight at 4°C with primary antibodies, diluted in blocking buffer. Primary antibodies used are listed in Table 1. The slides were then washed three times in 1x PBS, followed by incubation with Alexa Fluor-conjugated secondary

antibodies (1:1000 in blocking buffer; Invitrogen, Life Technologies, Grand Island, NY) for 30 minutes at room temperature. For DNA detection, we used DRAQ5 (1,5-bis{[2-(di-methylamino) ethyl]amino}-4, 8-dihydroxyanthracene-9,10-dione; Cell Signaling Technology, Danvers, MA; #4084). The secondary antibody cocktail was wicked off of the slide, replaced with DRAQ5 (1:3000 in blocking buffer), and incubated for 5 minutes. The slides were washed in 1x PBS three times and cover-slipped with Fluoromount-G (Southern Biotech, Birmingham, AL).

Protein extraction

Cortical tissue was excised from P0 littermates in ice cold 1x PBS, and kept on ice throughout the subsequent steps. The cortical tissue of each brain was dissociated by douncing in 5 times the tissue weight of lysis buffer (10 mM Tris, pH 7.5, 100 mM NaCl, 25 mM MgCl2, 0.5% NP40, protease inhibitor (complete ULTRA Tablets, Roche Applied Sciences, Indianapolis, IN)). Cultured cells were similarly rinsed in cold 1x PBS, scraped from the plate, and placed in 5 times the cell weight of lysis buffer. Dissociated cortical cells and cultured cells were processed identically in subsequent steps. The samples were vortexed for 30 seconds and placed on ice for 20 minutes. Nuclei were pelleted by centrifugation for 5 minutes at 10000 rpm. The supernatant was removed and replaced with 2 times the original tissue weight of lysis buffer with 0.5% Triton X-100. The nuclei were sonicated until the pellet dissolved; approximately 30 seconds. Membranes were pelleted by centrifugation and the nuclear extracts were used for western blot analysis or subsequent immunoprecipitation.

Expression plasmids

Epitope-tagged T7-TRA2A and T7-TRA2B expression plasmids were generated by cDNA amplification from mouse embryonic stem cells with specific primers for *Tra2a* or *Tra2b* that carry an XbaI or BamHI restriction site. These primers were: *Tra2a-XbaI*: 5’ GCGACTAGTAGTGATGTAGAGGAGAACAACTTCG 3’, *Tra2a-BamHI*: 5’ GCGGGATCCTCAATAGCGTCTTGGACTATAGGAA 3’, *Tra2b-XbaI*: 5’ GGCCACTAGTAGCGACAGCGGCGAGCAGAACTAC 3’, *Tra2b-BamHI*: 5’ GCGGGATCCTTAGTAGCGACGAGGTGAGTAGGA 3’. The PCR products were cut at the XbaI and BamHI sites and cloned into the pCGT7 expression vector (Cazalla et al., 2005; Wilson et al., 1995). The resulting plasmids consist of a T7-tagged TRA2A or TRA2B fusion protein under the control of the CMV promoter. The control (empty vector) plasmid is identical to pCGT7, except that the T7 sequence has been removed (Wilson et al., 1995).

Transfection

293T cells were grown to confluence in 10 cm dishes in Dulbecco's modified Eagle's medium (Gibco, Life Technologies, Grand Island, NY) with 10% fetal calf serum, at 37°C with 5% CO_2. Transfections were performed using lipofectamine 2000 (Invitrogen, Life Technologies) and 24 μg of plasmid DNA per plate. Transfection procedures followed the manufacturer's instructions. Transfected cells were cultured for 24 hours before harvesting.

Immunoprecipitation

Transfected cells were washed with 1x PBS and scraped from the plate. Nuclear protein extraction was performed as described above. Agarose immobilized T7 antibodies (Novagen, EMD Millipore, Billerica, MA; #69026-3) were washed 3 times with lysis buffer. The protein extract was then mixed with 20 μl of agarose T7-beads for 1 hour at 4°C. The beads were washed 3 times with lysis buffer before elution with 2x SDS-PAGE sample loading buffer (100 mM Tris pH 6.8, 0.25% glycerol, 2% SDS, 0.01% bromophenol blue,

0.05% β-Mercaptoethanol). The immunoprecipitates were denatured at 100°C for 5 minutes prior to SDS-PAGE.

Western Blot

Protein samples were resolved by 10% SDS-PAGE and transferred to a PVDF membrane in a Tris-Glycine (pH 8.8) buffer using the Genie Blotter system according to the manufacturer's directions (Idea Scientific Company, Minneapolis, MN). The membrane was blocked with 5% non-fat dried milk in TBST (20 mM Tris, 150 mM NaCl, 0.1% Tween 20) for 1 hour at room temperature. Blocked membranes were incubated with the primary antibodies in TBST overnight at 4°C (see Table 1 for antibody concentration). The membranes were washed with TBST three times and then incubated with horseradish peroxidase conjugated secondary antibodies (Santa Cruz Biotechnology, Santa Cruz, CA; 1:10,000 in TBST) for 1 hour at room temperature. After 3 washes with TBST, immune complexes were visualized by chemiluminesence (Super Signal West Pico, Thermo Scientific, Waltham, MA) according to the manufacturer's instructions, followed by exposure and development of autoradiography film (Santa Cruz Biotechnology, Santa Cruz, CA). To repeat the analysis with a different antibody, the membrane was stripped by a 30 minutes wash with 2 M Glycine, washed with TBST 3 times for 5 minutes each time, and re-blocked.

Antibody Characterization

Primary antibodies used for this study are listed in Table 1. Information on the production of these antibodies and their target specificity are described below.

BHLHB5 (class B basic helix-loop-helix protein 5, also known as BHLHE22, BETA3). Goat anti-BHLHB5 polyclonal antibody was raised against a KLH-conjugated 18 amino acid synthetic peptide mapping to a sequence within amino acid residues 2-19 of hamster BHLHB5 (ERGLHLGAAAASEDDLFL). This sequence shares 100% identity with mouse BHLHB5 amino acid residues 2-19. The specificity of anti-BHLHB5 was characterized by western blot analysis of rat lung and rat brain protein extracts. In both extracts the antibody recognized a band at 55 kDa, corresponding to endogenous BHLHB5 protein (manufacturer's technical notes; Santa Cruz Biotechnology, Santa Cruz, CA; sc-6045). Previously published immunohistochemistry using mouse brain sections has shown that the anti-BHLHB5 antibody stains the nuclei of cortical neurons in layers 2-5, and that this staining is lost in a BHLHB5 knockout mouse (Joshi et al., 2008). In the current study, the anti-BHLHB5 antibody was used to identify projection neurons in cortical layers 2-5. This allowed us to establish co-localization with TRA2B, and compare projection neuron numbers and location between the *Tra2b cKO* and control mice.

Cleaved Caspase-3. Activation of Caspase-3 requires proteolytic cleavage of the full-length protein at Asp175 to produce activated fragments p17 and p19 (Nicholson et al., 1995). Rabbit anti-cleaved Caspase-3 polyclonal antibody was produced using a KLH-conjugated synthetic peptide immunogen corresponding to the 13 amino acids at the C-terminus of p17/19 (CRGTELDCGIETD). The cleaved Caspase-3 antibody was characterized by western blot analysis of HeLa (human), NIH/3T3 (murine fibroblasts), and C6 (rat glia) cell extracts. Under normal conditions the antibody detected little or no protein at 17/19 kDa. Following treatment of cells with Staurosporine or Cytochrome C (to promote apoptosis) bands at 17 and 19 kDa were clearly detected. The full-length inactive Caspase-3 protein was not recognized by this antibody on western blot. The specificity of the cleaved Caspase-3 antibody was confirmed by immunohistochemistry of cultured cells and tissue sections. Staining with anti-cleaved Caspase-3 antibody labeled etoposide-treated Jurkat cells, while untreated cells were sparsely labeled. This antibody also detected cleaved

Caspase-3$^+$ cells in mouse embryo sections. This recognition was blocked by pre-absorption with a cleaved Caspase-3 blocking peptide (Cell Signaling Technology, Danvers, MA; 1050) and unaffected by pre-absorption with a control peptide (manufacturer's technical notes; Cell Signaling Technology, Danvers, MA; 9661). We have previously identified apoptotic cells in mouse tissue sections using anti-cleaved Caspase-3 (Eckler et al., 2011). Here we use anti-cleaved Caspase-3 to identify apoptotic cells in *Tra2b cKO* and control brains.

CTIP2 (also known as BCL11B, B-cell leukemia/lymphoma 11B). Anti-CTIP2 (clone 25B6) is a rat monoclonal antibody that recognizes the N-terminus of CTIP2. The immunogen used was a GST-CTIP2 fusion protein, consisting of the full-length human CTIP2 (amino acids 1-812). The epitope has been mapped to exon 2 (amino acids 19-127). The specificity of the anti-CTIP2 antibody was characterized by immunohistochemistry and western blot analysis. Western blot analysis of mouse brain lysate produced two bands at 100 and 110 kDa corresponding to the two CTIP2 isoforms. The anti-CTIP2 antibody recognized cultured hippocampal cells and tissue sections by immunohistochemistry (manufacturer's technical notes; Abcam, Cambridge, MA; ab18465). In previous studies we have shown that the anti-CTIP2 antibody specifically labels the nuclei of subcerebral and corticothalamic projection neurons in cortical layers 5 and 6 (Chen et al., 2008; McKenna et al., 2011). The signals detected by western blot and immunohistochemistry were lost in *Ctip2* knockout mice (Wakabayashi et al., 2003). In this report we use anti-CTIP2 to identify subcortical projection neurons. This localization is used to establish co-localization with TRA2B and to identify changes in cortical projection neuron populations in the *Tra2b cKO*.

EWS (Ewing sarcoma breakpoint region 1 protein). The mouse monoclonal antibody, anti-EWS (clone C-9), was raised against a KLH-conjugated peptide mapping to amino acids 2-43 of human EWS (ASTDYSTYSQAAAQQGYSAYTAQPTQGYAQTTQAYGQQSYGT). Using western blot analysis, anti-EWS recognized EWS as a 90 kDa band in K-562 and F9 (human) whole cell lysates, and rat testis extract. Anti-EWS localizes specifically to nuclei in HeLa (human) cells, human pancreatic tissues, porcine fibroblasts, and porcine neural progenitor cells by immunohistochemistry (Blechingberg et al., 2012; manufacturer's technical notes; Santa Cruz Biotechnology, Santa Cruz, CA; sc-48404). In this study we use the anti-EWS to detect EWS protein, which is used as western blot loading control for whole cell lysates.

GFP (green fluorescence protein). Production of the chicken anti-GFP antibody was achieved using purified recombinant EGFP as the immunogen. This antibody did not detect specific signals in western blot or immunohistochemical analyses of wild type mice because GFP was not endogenously expressed. The anti-GFP antibody was able to detect GFP by western blot analysis of protein extracts from GFP-expressing transgenic mice. It also detected tissue-specific GFP expression in immunohistochemical analysis of these transgenic animals (manufacturer's technical notes; Aves Labs, Tigard, OR; GFP-1020). Our previously published results show that this antibody specifically identified GFP$^+$ cells with the expected position and morphology (Eckler et al., 2011). In this report, the GFP antibody was used to label GFP-expressing cortical cells and their axons in *RCE-GFP* CRE reporter mice.

SOX2 (SRY-box containing gene 2). The goat anti-SOX2 antibody was generated using a KLH-conjugated synthetic peptide corresponding to amino acids 277-293 of human SOX2 (YLPGAEVPEPAAPSRLH). This sequence is identical to residues 279-295 of mouse SOX2. The antibody was characterized by western blot on human and mouse embryonic stem cell lysates, and detected SOX2 protein in both lysates as a single band at 34 kDa. Immunohistochemical analysis on mouse embryonic stem cells showed that this antibody

stained a nuclear localized protein (manufacturer's technical notes; Santa Cruz Biotechnology, Santa Cruz, CA; sc-17320). The anti-SOX2 antibody does not normally stain mouse mesenchymal stem cells, but upon transfection with a *Sox2* cDNA these cells were stained by the antibody (Ding et al., 2012). Conversely, human embryonic stem cells showed strong staining with this antibody, and the signal was disrupted when the cells were treated with Sox2 siRNA (Adachi et al., 2010). In our experience, this anti-SOX2 antibody recognizes cells identical in morphology and position to SOX2-expressing cells characterized in previous reports (Hutton and Pevny, 2011). For our study, this SOX2 antibody is used to identify cortical progenitors in the ventricular zone.

T7 (T7 bacteriophage gene 10). In this study we used two different T7 antibodies. The first anti-T7 polyclonal antibody was produced in rabbits immunized with a KLH-conjugated T7 epitope (MASMTGGQQMG). By western blot analysis, anti-T7 is able to detect exogenously expressed T7 fusion protein as a single band (manufacturer's technical notes; Bethyl Laboratories, Montgomery, TX; A190-117A). In this study anti-T7 is employed for western blot detection of T7 epitope fusion proteins.

The second T7 antibody used in this report is anti-T7-agarose. This is a mouse monoclonal antibody directed against the 11 amino acid T7-tag (MASMTGGQQMG), coupled to agarose beads (Novagen, EMD Milipore, Billerica, MA; 69026-3). Anti-T7-agarose has been successfully used for immunoprecipitaion of T7-tagged protein (Hayakawa et al., 2007). In this report we use anti-T7-agarose for immunoprecipitation of T7 epitope fusion proteins.

TBR1 (T-box brain 1). The rabbit anti-TBR1 antibody was produced using a KLH-conjugated synthetic peptide epitope mapping to residues 65-82 of mouse TBR1 (TDNFPDSKDSPGDVQRSK). Western blot analysis using this antibody shows specific staining of a 74 kDa band at the expected size of endogenous TBR1, in mouse and rat hippocampal lysates. By immunohistochemistry, this antibody specifically stains individual nuclei of cultured rat neurons and tissue sections of mouse and human cerebral cortex (manufacturer's technical notes; Abcam, Cambridge, MA; ab23345). Specific staining of corticothalamic neurons and some layer 5 neurons has been observed using this antibody in the mouse cerebral cortex (McKenna et al., 2011), consistent with *Tbr1* mRNA expression patterns established by *in situ* hybridization, and staining with alternative TBR1 antibodies (McKenna et al., 2011; Rubenstein et al., 1999). We use the TBR1 antibody to identify changes in the number and location of cortical corticothalamic neurons in the *Tra2b cKO* mouse.

TRA2A (transformer 2 homolog alpha). Anti-TRA2A is a mouse monoclonal antibody raised against GST-conjugated full-length human TRA2A. Using western blot analysis, anti-TRA2A detected a specific band in TRA2A-tranfected 293T (human) cell lysate, but did not produce a signal in un-transfected 293T cell lysate. Anti-TRA2A also recognized a band of ~33 kDa in HepG2 (human) cell lysate. By immunohistochemistry of HeLa cells, anti-TRA2A produced a nucleus specific staining pattern (manufacturer's technical notes; Sigma-Aldrich, St. Louis, MO; SAB1400517). In this study we use western blot analysis with anti-TRA2A to confirm the specificity of anti-TRA2B.

TRA2B (transformer 2 homolog beta, also known as SFRS10). The anti-TRA2B antibody was generated by immunizing rabbits with a synthetic peptide corresponding to the N-terminal 15 amino acids of human TRA2B protein (MSDSGEQNYGERESR) as previously described (Hofmann and Wirth, 2002). This peptide sequence is conserved between human and mouse TRA2B, making the antibody useful for identifying TRA2B in either species. The resulting polyclonal antibody was characterized by western blot analysis of both

endogenous and recombinant TRA2B in HEK293 (human) and NIH/3T3 (murine fibroblast) cells. Endogenous TRA2B was identified as a band at 40kDa, while the larger recombinant TRA2B was detected as a separate band (Hofmann and Wirth, 2002). Specificity of the anti-TRA2B antibody was confirmed by immunohistochemistry and western blot analysis. The anti-TRA2B antibody detected ubiquitous TRA2B expression in the early embryo but this staining was lost upon knockout of *Tra2b*. In western blot analysis, decreased TRA2B level was observed in the *Tra2b* heterozygous knockout mouse when compared to a wild type control (Mende et al., 2010).

The TRA2B antibody we used has been previously published and characterized, but reactivity with the closely related TRA2A was not tested (Grellscheid et al., 2011; Mende et al., 2010). The specificity of the TRA2B antibody was confirmed by western blot analysis of T7 epitope tagged-TRA2A and T7-TRA2B in transiently transfected HEK293T cells (Figure 1). Control cells, transfected with empty vector showed no cross-reactivity with the T7 antibody. By contrast, cells transfected with either T7-TRA2A or T7-TRA2B revealed a band of ~40 kDa which strongly cross-reacts with the T7 antibody (Figure 1, upper panel compare lane 1 with 2 and 3). Both T7-TRA2A and T7–TRA2B can be immunoprecipitated from lysates prepared from transfected cells but not control cells (Figure 1, upper panel, compare lane 4 with 5 and 6). Parallel blots were probed with antibodies against TRA2A, TRA2B and EWS. Anti-TRA2A only recognized exogenously expressed T7-TRA2A in both the input extracts and immunoprecipitates. By contrast, anti-TRA2B recognized both endogenous TRA2B and exogenous T7-TRA2B (Figure 1, compare lanes 1-3 and open and black arrow heads, respectively). Anti-TRA2B also recognized immunoprecipitated T7-TRA2B but not T7-TRA2A. Finally, the unrelated EWS protein was present in all three input extracts, but absent from the immunoprecipitates, confirming the specificity of the anti-T7 immunoprecipitation. Taken together, these results demonstrate that TRA2B antibody raised against the N-terminal peptide (MSDSGEQNYGERESR) is specific for TRA2B and shows no appreciable cross-reactivity with TRA2A. In this report we use this TRA2B antibody to investigate the spacial and temporal expression of TRA2B.

U2AF65 (U2 auxiliary factor 65 kDa subunit). The mouse anti-U2A65 (clone MC3) monoclonal antibody was generated with full-length recombinant human U2AF65 as the antigen. As a positive control, this antibody recognizes a 65 kDa target in western blot analysis of HeLa (human) whole cell lysate and Jurkat (human), SK-N-MC (human), and KNRK (rat) nuclear extracts (manufacturer's technical notes; Santa Cruz Biotechnology, Santa Cruz, CA; sc-53942). U2AF65 has been shown to function in U2-type intron splicing, and is not required for U12-intron splicing (Graveley et al., 2001; Shen and Green, 2007). Upon isolation and western blot of the U2-type spliceosome and the U12-type spliceosome, anti-U2AF65 recognized U2AF65 exclusively in the U2-type spliceosome (Shen et al., 2010). Anti-U2AF65 antibody has been previously used to identify U2AF65 as a western blot loading control (Izquierdo and Valcárcel, 2007). In this study we also use anti-U2AF65 as a loading control for western blot analysis.

PLAP (placental alkaline phosphatase) staining

Fezf2-PLAP brains were fixed as described for immunohistochemistry. After overnight cryoprotection with 30% sucrose they were sliced into 50μm floating sections in 1x PBS. The sections were post-fixed for 1 hour in 4% PFA, washed with 1x PBS three times for 5 minutes each, and incubated in 1x PBS at 70°C for one hour. They were then washed at room temperature with staining buffer (100 mM Tris, 50 mM NaCl) and incubated with AP substrate (0.5 mg/ml nitroblue tetrazolium, 0.1 mg/ml 5-bromo-4-chloro-3-indolyl phosphate in 100 mM Tris, 50 mM NaCl) at 37°C until color developed. Excess stain was

washed off with PBST (0.5% Triton x-100 in 1x PBS) and sections were mounted onto slides and cover-slipped.

In situ hybridization

The *Nrp2* (neuropilin 2) probe sequence was chosen according to the sequence used by the Allen Institute for Brain Science (http://mouse.brain-map.org/experiment/show?id=80514091). Probe templates were amplified from mouse brain cDNA by nested PCR using three primers: forward, reverse, and nested primers. The first round of PCR used the forward and reverse primers, with the following sequences: *Nrp2*-forward: 5' GGGGTGAAGAATGGCTTCAGGTAG 3', *Nrp2*-reverse: 5' TACTCCATGTCATAGCTGGGC 3'. The PCR product was gel-purified, and used as the template for a second round of PCR using the forward primer and nested primer. The sequence for the nested primer was identical to the reverse primer sequence conjugated, at the 5' end, to the SP6 promoter sequence. Sp6-*Nrp2*-reverse: 5' GATTTAGGTGACACTATAGTACTCCATGTCATAGCTGGGC 3'. The sequence of the PCR product was confirmed by sequencing with the *Nrp2*-forward and Sp6 primer: 5' GATTTAGGTGACACTATAG 3'.

In vitro transcription reactions were performed using the 10x DIG RNA Labeling Mix (Roche Applied Sciences, Indianapolis, IN) in accordance with the manufacturer's instructions. Template DNA was removed by digestion with DNase I (New England Biolabs, Ipswich, MA) and RNA probes were purified using Centri-sep spin columns (Invitrogen, Life Technologies, Grand Island, NY). Purified probes were diluted to 50 μg/ml in hybridization buffer (AMRESCO, Solon, OH; 0973), aliquoted, and frozen for storage.

Brains were fixed and sectioned onto slides at 20 μm, as described for immunohistochemistry. Sections were post-fixed in 4% PFA for 10 minutes, washed 3 times in 1x PBS for 5 minutes each time, acetylated for 10 minutes (1.5% triethanolamine, 0.175% HCl, 0.25% acetic anhydride), and washed 3 times in 1x PBS for 5 minutes each time. Slides were incubated in hybridization buffer (AMRESCO, Solon, OH; 0973) for 2 hours, and hybridized with the denatured RNA probe (250 ng/ml labeled RNA in hybridization buffer; heated at 80°C for 5 minutes, then placed on ice) overnight at 70°C. After a brief wash in 70°C 5x SSC (0.75 M NaCl, 0.075 M sodium citrate; pH 7.0), slides were incubated in 0.2x SSC at 70°C for 2 hours, RNAse buffer (0.5 M NaCl, 10 mM Tris pH 7.5, 5 mM EDTA) at 37°C for 5 minutes, and with 10 μg/ml RNAse A (Invitogen, Life Technologies, Grand Island, NY) in RNAse buffer at 37°C for 30 minutes. The slides were washed in RNAse buffer at 37°C for 5 minutes, followed by incubation in 0.2x SSC at 70°C for 1 hour. Slides were moved to room temperature 0.2x SSC for 5 minutes, buffer B1 (0.1 M Tris pH 7.5, 0.15 M NaCl) for 5 minutes, buffer B2 (1% heat inactivated goat serum in buffer B1) for 1 hour, and incubated overnight with AP-conjugated anti-DIG antibody (1:5000 in buffer B2; Roche, #11093274910) at 4°C. Slides were washed 3 times (5 minutes/wash) in buffer B1, 5 minutes in staining buffer (100 mM Tris, 50 mM NaCl), and incubated with AP substrate (0.5 mg/ml nitroblue tetrazolium, 0.1 mg/ml 5-bromo-4-chloro-3-indolyl phosphate; in 100 mM Tris, 50 mM NaCl). After color had developed sufficiently, slides were washed in water and cover-slipped with Permount (Fisher Chemical, Fairlawn, NJ).

Microscopy

Bright field and epifluroscence images of tissue sections were collected on a Biorevo BZ-9000 light microscope (Keyence America, Elmwood Park, NJ). Images of the cerebral cortex alone were collected on a Leica TCS SP5 confocal microscope (Leica Microsystems, Buffalo Grove, IL). Brightness, contrast, and color channels were adjusted using Photoshop CS5 software (Adobe Systems Inc., San Jose, CA). For each image presented in the figures,

a minimum of three different brains ($n \geq 3$) of each genotype and age were examined to confirm epifluorescent or enzymatic staining patterns.

Quantification and statistics

Quantities quoted in the text are in the form of mean ± standard deviation (SD). Bar graphs similarly represent mean with error bars indicating SD. *P*-values were determined by a two-tailed student's t-test. Values with $P < 0.05$ were considered significantly different. $P < 0.005$ was considered very significantly different and denoted by a triple star (***) on graphs. Individual cell counting was performed manually using images taken on the Leica SP5 confocal microscope. These images were taken from coronal sections as shown in Figures 1A, 1E, and 1I. A 200 μm width of cortex, at the location shown in Figures 1B, 1F, and 1J, was used for quantification. Manual cell counting was performed on three adjacent medial sections per brain, and averaged. Values presented in the text result from analysis three brains (n = 3) per age and genotype. At E11.5, E15.5, and P0, 2166, 2265, and 2032 $SOX2^+$ progenitor cells were counted, respectively. From P0 sections, a total of 2675 $CTIP2^+$ and 2720 $BHLHB5^+$ cells were counted. Upon quantification of $CC3^+$ nuclei we identified a total of 3383 apoptotic cells from *Tra2b cKO* sections and 17 apoptotic cells in matched control sections.

Area and length measurements were generated by the Keyence light microscope and the BZ-II Analyzer software (Keyence America, Elmwood Park, NJ). Images of P0 brains probed by *in situ* hybridization for *Nrp2* were used to obtain these measurements. These brains were sectioned such that each slide contains a 20 μm coronal slice from every 200 μms along the rostral-caudal axis of the cerebral cortex. For each brain, images of all sections on a single slide were taken. The area of the cortex in each section was manually delineated to allow quantification by the BZ-II Analyzer software. The total volume of the cerebral cortex was obtained by extrapolating from area measurements by Cavalieri's method (Vaccarino et al., 1999). This method determines volume using the following equation: $V = \sum 2A*t$. A is the area of a single cortical hemisphere in a single section. This is multiplied by 2 to find the area of the entire cortex in a single section. t is the thickness of each sample. The brains were sliced into 20 μm sections onto 10 slides. Because we imaged a single slide, each slice represents $t = 20\mu m \times 10$. To calculate the total volume, the volume represented by each section on the slide was summed. Volume calculations were done for 3 control and 3 *Tra2b cKO* brains.

We chose matched coronal sections at the anterior-posterior position indicated by a dotted line in Figure 4D to quantify the length of cortical domains. The cortical domains of these matched sections were manually outlined as shown by dotted lines in Figures 4A and 4B. Solid lines in Figures 4A and 4B show the boundary between the neocortex and piriform cortex. Lines were traced on the basal surface of the cortex over the regions occupied by the piriform cortex and neocortex. The length of these lines was then measured by the BZ-II Analyzer software. Cortical domain lengths were measured from 3 control and 3 *Tra2b cKO* brains.

Results

TRA2B is expressed in neural progenitors and projection neurons during cortical development

Previous studies indicated that TRA2B is expressed in the embryonic cerebral cortex (Grellscheid et al., 2011), but the specific temporal and spacial expression patterns within the cortex were not determined. We defined the pattern of TRA2B expression in wild-type brains during cortical neurogenesis. Immunohistochemical analysis using antibodies against

TRA2B and other cell type markers on brains collected from E11.5 to P0 showed that TRA2B protein was detected throughout the brain, with robust expression in the developing cerebral cortex (Figure 2). At E11.5, the start of cortical neurogenesis, TRA2B was expressed in both the ventricular zone (VZ) and the preplate (Figure 2A-D). Most of the $SOX2^+$ radial glial cells at the VZ expressed TRA2B (Figure 2A-D). At E15.5 (Figure 2E-H) and P0 (Figure 2I-R), TRA2B expression was observed in both the VZ and the cortical plate. Quantitative analysis showed that TRA2B was expressed in almost all SOX2-expressing neural progenitors. In the VZ, TRA2B was detected in 97.8 ± 0.5% of SOX2-expressing cells at E11.5, 96.6 ± 3.7% at E15.5, and 96.3 ± 1.2% at P0.

We used CTIP2 and BHLHB5 as markers for cortical projection neurons, and examined neuronal expression of TRA2B. CTIP2 is normally expressed in layer 5 and 6 cortical projection neurons, with a higher expression level in layer 5 than in layer 6 (Figure 2M, O). BHLHB5 is expressed in projection neurons in layers 2-5 (Figure 2P, R). The combined expression patterns of CTIP2 and BHLHB5 identify many postmitotic neurons across layers 2-6 of the cerebral cortex. TRA2B was expressed in both CTIP2 and BHLHB5-expressing projection neurons (Figure 2M-R). At birth, TRA2B expression was observed in 93.6 ± 4.9% of CTIP2-expressing cells, and 95.6 ± 0.4% of BHLHB5-expressing cells. TRA2B expression in cerebral cortex neurons persists at least two weeks after birth (data not shown). The broad TRA2B expression observed in neural progenitors and in cortical projection neurons throughout cortical development suggests its potential involvement in regulating neural progenitor and cortical neuron survival, proliferation, or differentiation.

Tra2b cKO mice have a reduced and disorganized cortex

Ubiquitous knockout of TRA2B in mice has been shown to be embryonic lethal (Mende et al., 2010), demonstrating that TRA2B is essential during mammalian embryogenesis. Based on the broad TRA2B expression observed in the developing cerebral cortex (Figure 2), we sought to determine the function of TRA2B in cortical development. To circumvent the early lethality caused by the *Tra2b* mutation, we utilized a floxed *Tra2b* allele. Mice containing this allele were bred with those harboring an *Emx1-cre* allele, to generate cortex-specific *Tra2b* conditional mutant mice (*cKO*). The *Emx1-cre* allele drives CRE recombinase expression in postmitotic neurons and neural progenitors of the developing cerebral cortex as early as E9.5, and recombination has been observed in more than 88% of the mature neurons (Gorski et al., 2002). Thus, in $Emx1^{cre/+}$; $Tra2b^{fl/fl}$ mice, *Tra2b* is removed from both neural progenitors and neurons.

To identify the effects of *Tra2b cKO* on the development of the cerebral cortex, we first examined the brains on P0 (Figure 3). Comparisons between control and *Tra2b cKO* littermates showed that, at this age, the majority of cerebral cortex and hippocampus structures were missing in the *Tra2b cKO* (Figure 3A-D). The midbrain, hindbrain, and ventral forebrain were not apparently affected in these animals (Figure 3A-D). Despite this dramatic phenotype, *Tra2b cKO* mice survive to adulthood and do not exhibit gross behavioral abnormalities.

To investigate how different types of cortical projection neurons were affected in the *Tra2b cKO* brains, we performed immunohistochemical analysis using projection neuron subtype specific markers CTIP2, BHLHB5, and TBR1 (Figure 3C-N). In control brains, TBR1 was expressed in corticothalamic neurons that were located in layer 6, and low-level TBR1 expression was also detected in layers 2/3 (Figure 3E-G). CTIP2 was expressed in neurons in layers 5 and 6 (Figure 3E, F, H), and BHLHB5 was expressed in layers 2-5 (Figure 3E, F, I). Immunohistochemical analysis of *Tra2b cKO* brains revealed that the caudal and medial parts of the cortex were missing (Figure 3D, J). In the rostral and lateral regions of the cortex, parts of the cerebral cortex remained, but a reduction in cortical plate thickness was

observed, and the numbers of $TBR1^+$, $CTIP2^+$ and $BHLHB5^+$ cells were reduced (Figure 3E-N). The general distinction of cortical layers could be identified, however the cortical layers were disorganized, and boundaries between different layers were indistinct (Figure 3E-N). In control brains, layers 2/3 can be identified by the low-level expression of TBR1 and BHLHB5 (Figure 3E, F, G, I). In the *Tra2b cKO* brains, layer 2/3 neurons were barely detectable (Figure 3J, K, L, N).

Even though the six-layered neocortex was smaller and thinner, the three-layered piriform cortex did not appear to be as severely affected in the *Tra2b cKO* brains (Figure 3E, J). To confirm whether this was the case, we performed *in situ* hybridization for the *Nrp2* gene to identify the piriform cortex (Figure 4A, B) (Chou et al., 2009). We measured the length of the cerebral cortex, neocortex, and piriform cortex along the pial surface (Figure 4A, B) in matched coronal brain sections, at the indicated anterior-posterior position (Figure 4D). We also calculated the volume of the cerebral cortex for both control and *Tra2b cKO* brains. Although the volume of the *Tra2b cKO* cortex was reduced when compared to control littermates, and the length of both cerebral cortex and neocortex were significantly decreased, we observed no significant change in the absolute length of the piriform cortex in *Tra2b cKO* brains (Figure 4C, E). The volume of the *Tra2b cKO* cortex was reduced to 30.2 ± 9.0% that of control littermates, from 13.1 ± 1.0 mm^3 in the control to 4.0 ± 0.5 mm^3 in the *Tra2b cKO*. The length of the total cerebral cortex decreased from 5.0 ± 0.2 mm in the control to 2.8 ± 0.3 mm in the *Tra2b cKO*. The decrease in total cortex length was primarily due to the difference between neocortical lengths in the control and *Tra2b cKO* (4.0 ± 0.1 mm and 1.5 ± 0.2 mm respectively), as we observed no significant difference in the length of the piriform cortex (1.1 ± 0.1 mm in the control and 1.3 ± 0.2 mm in the *Tra2b cKO*; Figure 4E). These measurements indicated that the piriform cortex had developed normally.

We hypothesized that the rostral and lateral regions of the cerebral cortex were spared in the *Tra2b cKO* brains due to inefficient TRA2B knockout in these regions. To test this possibility we performed immunohistochemistry using antibodies against TRA2B (Figure 5A-H). At E11.5 we observed a visible reduction in TRA2B expression in the *Tra2b cKO* cerebral cortex (Figure 5A-D), consistent with the expected knockout from *Emx1*-CRE expression. At P0, TRA2B was expressed in cortical neurons of the control brains (Figure 5E, F). In the *Tra2b cKO* brains, TRA2B expression was reduced but still observed in many cells in the remaining cortex (Figure 5G, H). Western blot analysis of these P0 brains confirms that TRA2B expression is reduced in the *Tra2b cKO* cortices (Figure 5I). These results demonstrated that CRE-mediated recombination had not occurred or was incomplete in some cortical cells, but that TRA2B expression decreased overall. Inefficient recombination of *Tra2b* may be partially responsible for sparing the rostral and lateral cortical regions.

Axons from cortical projection neurons are decreased in the *Tra2b cKO* brains

We next determined how the axons of cortical projection neurons were affected in the *Tra2b cKO* brains. We used two complementary genetic strategies to label the cortical axons. *Fezf2* is a gene that is specifically expressed in subcerebral and corticothalamic projection neurons (Chen et al., 2005 a; b; Molyneaux et al., 2005; Chen et al., 2008; Han et al., 2011; McKenna et al., 2011). Previously a *Fezf2-PLAP* allele was generated in which a PLAP gene was inserted into the *Fezf2* gene locus to label subcerebral and corticothalamic axons (Chen et al., 2005 a). We crossed the *Fezf2-PLAP* allele into the *Tra2b cKO* mice and compared PLAP-labeled axons in *Emx1-cre;* $Tra2b^{fl/+}$*;* $Fezf2^{PLAP/+}$ (control) and *Emx1-cre;* $Tra2b^{fl/fl}$*;* $Fezf2^{PLAP/+}$ (*cKO*) mice (Figure 6). In the control brains, PLAP-labeled axons were present in the striatum (Figure 6C), internal capsule (Figure 6G), anterior commissure (Figure 6E), thalamus (Figure 6I), cerebral peduncle (Figure 6K), and

pyramidal tract (Figure 6A). In the *Tra2b cKO* brains, the corpus callosum was missing (Figure 6D), and far fewer PLAP-labeled axons were observed in the striatum (Figure 6D) and internal capsule (Figure 6H). PLAP-labeled axons were not detected in the thalamus (Figure 6J), cerebral peduncle (Figure 6L), or pyramidal tract (Figure 6B).

We utilized an alternative strategy to label all of the axons from the cortical projection neurons in the control and *Tra2b cKO* mice (Figure 7). We generated *Emx1-cre; Tra2b*$^{fl/+}$*; RCE-GFP* (control) and *Emx1-cre; Tra2b*$^{fl/fl}$*; RCE-GFP* (*cKO*) mice. The *RCE-GFP* transgene is a reporter allele that upon CRE-mediated recombination allows GFP expression, labeling both cell bodies and axons of the affected cells. In the control brains, GFP-labeled cortical axons were observed in the corpus callosum (Figure 7A), striatum (Figure 7A, I), internal capsule (Figure 7A, C, E; identified with an asterisk), and projecting into the thalamus (Figure 7E, J). GFP-labeled axon bundles were also visible in the cerebral peduncle, projecting toward the brain stem and spinal cord (Figure 7G). Similar to what has been observed with the *Fezf2-PLAP* axonal marker, few GFP-labeled cortical axons were present in the internal capsule (Figure 7B, D, F, K), or projecting toward the thalamus (Figure 7F, L). Far fewer GFP+ axons were observed in the cerebral peduncle in the mutant brains (Figure 7H). Together, the results from these two axon labeling strategies showed that in the absence of TRA2B function, both callosal axons and subcortical axons were severely defective.

Apoptosis of neural progenitors in the *Tra2b cKO* mouse

The reduced cortical sizes in the *Tra2b cKO* brains suggested that TRA2B was required for either the proliferation or survival of the cortical progenitors and neurons. To distinguish between these possibilities and determine when the reduced cortical size could first be detected, we examined the *Tra2b cKO* brains at embryonic stages. We performed immunohistochemistry using antibodies for cleaved Caspase-3 (CC3; Figure 8) to identify apoptotic cells (Riedl and Salvesen, 2007). At E10.5, the size and thickness of the cortices in the *Tra2b cKO* mice did not appear significantly different from the control mice (Figure 8A, E). However, scattered $CC3^+$ cells were detected in the dorsal regions of the cortex in the *Tra2b cKO* brains (Figure 8E). This is also the earliest stage we observed increased CC3 staining in the *Tra2b cKO* brains. One day later, at E11.5, neurogenesis has begun in the cerebral cortex, but most of the cortical cells are still neural progenitors (O'Leary and Nakagawa, 2002; Hutton and Pevny, 2011). $CC3^+$ cells were rare in the control brains (Figure 8B), but extensive apoptosis was observed throughout the developing cerebral cortex in the *Tra2b cKO* mice (Figure 8F). Quantitative analysis showed a 198-fold increase in the number of $CC3^+$ cells in the *Tra2b cKO* cortices over those in control cortices at E11.5. In the control brain we counted 1.9 ± 0.3 $CC3^+$ nuclei in a 200 μm width of cortex, compared to 375.9 ± 75.7 $CC3^+$ nuclei in the *Tra2b cKO* representing a very significant increase ($P<0.001$). These numbers represent a conservative estimation of the number of apoptotic cells in the *Tra2b cKO*. Due to the density of staining in the mutant cortices only $CC3^+$ cells with a single intact nucleus were counted, excluding those cells at later stages of apoptosis with fragmented nuclei. At E12.5, the cerebral cortex in the *Tra2b cKO* was visibly reduced in size compared to the control littermate, and the lateral ventricles had begun to collapse (Figure 8C, G). Widespread CC3 staining continued to be detected at E12.5 (Figure 8G). By E15.5, the dorsal and medial regions of the cerebral cortex had disappeared in the *Tra2b cKO* brains. The chorus plexus was directly connected to the lateral cortical region, the lateral ventricles had collapsed, and ectopic apoptosis was no longer detectable (Figure 8D, H). This result showed that TRA2B is required for the survival of cortical progenitor cells.

Discussion

Alternative splicing increases transcript diversity and is an efficient way to regulate gene function. However the importance of alternative splicing factors in brain development has not been investigated. Mammalian TRA2B is a RS domain-containing protein that regulates alternative splice site selection through binding to exonic splicing enhancers (Long and Caceres, 2009; Shepard and Hertel, 2009; Grellscheid et al., 2011). TRA2B and its homologs are important in a wide variety of developmental processes. Here, we examined the function of TRA2B in the development of the cerebral cortex by investigating its expression patterns and the phenotype of cortex-specific *Tra2b cKO* mice. We have observed that TRA2B is expressed in both radial glial cells and postmitotic projection neurons during cortical neurogenesis. In the *Tra2b cKO* mice, neural progenitor cells quickly degenerated, resulting in a cortex missing the posterior and medial regions at birth. Thus, our results demonstrate that TRA2B is essential for the survival of cortical neural progenitor cells.

Immunohistochemistry shows that TRA2B is expressed broadly in both radial glial cells and cortical projection neurons, suggesting that it is an important regulator in cortical development. Indeed, in the cortex-specific *Tra2b cKO* mice, extensive death of neural progenitor cells begins in the medial cortical regions at E10.5, and proceeds quickly toward more lateral regions. By E15.5, the chorus plexus is directly connected to the lateral neocortex. The rapid apoptosis of affected neural progenitors precludes later analysis of these *Tra2b cKO* cells. We currently don't know the mechanisms underlying the survival of progenitors and neurons in the lateral region, but there are several potential reasons. First, within the developing cortex, *Emx1* is expressed in a posterior-medial high and anterior-lateral low gradient (Gulisano et al., 1996). It is highly likely that *Emx1-cre* is also expressed in such a gradient, and results in incomplete deletion of TRA2B in the anterior and lateral cortical regions. Indeed, in the *Tra2b cKO* brains, TRA2B protein was still detected in some of the surviving cortical cells (Figure 5E-H). Second, many SR and SR-related proteins are expressed in the developing cortex during mid-cortical neurogenesis (Figure 9; Visel et al., 2004; Diez-Roux et al., 2011). For example, *Sfrs2ip* (Figure 9B), *Sfrs6* (Figure 9D), and *Sfrs9* (Figure 9G) are expressed in the ventricular zone, while *Psip1* (Figure 9A), *Sfrs3* (Figure 9C), *Sfrs7* (Figure 9E), *Sfrs8* (Figure 9F), *Sfrs11* (Figure 9H), and *Sfrs14* (Figure 9I) are expressed in both the ventricular zone and the cortical plate. The broad expression of these genes not only suggests that alternative splicing mediated by these factors is important for the development of the cerebral cortex, but also that they may compensate for the loss of TRA2B function, allowing some of the *Tra2b cKO* cells to persist.

In addition to apoptosis of cortical progenitor cells, our results revealed extensive cortical disorganization and axonal defects in the *Tra2b cKO* mice. These defects could be an indirect result of wide-spread apoptosis of cortical progenitor cells, or TRA2B may also directly regulate neuronal migration and differentiation. TRA2B was shown to regulate alternative splicing of exon 7 of *SMN1* and *SMN2.* SMA results from mutation of *SMN1*, so the severity of SMA is dependent on correctly spliced *SMN2* pre-mRNA, influenced by TRA2B (Hofmann et al., 2000; Wirth et al., 2013). TRA2B was also shown to influence *Tau* alternative splicing, which results in neurodegeneration and dementia when mis-regulated (Wang et al., 2005). These specific TRA2B targets manifest phenotypic defects in terminally differentiated neurons, so a reasonable hypothesis is that TRA2B regulates alternative splicing of genes involved in the differentiation, migration, maturation, or maintenance of cortical neurons. Examination of neuron-specific *Tra2b cKO* mice will be helpful in determining its function in postmitotic neurons.

The broad expression of SR and SR-related proteins during cortical neurogenesis suggests the importance of alternative splicing in regulating protein expression during this process. While much effort has been undertaken to understand transcription factors and signaling molecules in regulating the generation of the cerebral cortex, few attempts have been made to determine the roles of alternative splicing regulators in cortical development. Our analysis of the cortex-specific *Tra2b cKO* brains has begun to reveal the importance of alternative splicing for cortical progenitor cell survival. Future studies should be directed toward identifying the splicing targets of TRA2B in the developing cortex and understanding the functions of other alternative splicing regulators.

Acknowledgments

This work was funded by R01MH082965 (to BC) and GM085121 (to JS) from the National Institute of Health , a New Faculty Award RN1-00530-1 (to BC) and a Training Award TG2-00157 (to HE) from the California Institute of Regenerative Medicine (CIRM), and Center for Molecular Medicine Cologne grant No D5 (to BW). Additional support was provided by the Ellison Foundation for Medical Research and Center for Computational and Applied Transcriptomics (University of Copenhagen) (to JS). We thank Jon Howard, Brian Sumstine, and Sol Katzman for providing technical expertise and assistance over the course of this study. We also thank members of the Chen Lab, Feldheim Lab, Sanford Lab, and Ares Lab for helpful discussion during the execution of these experiments.

Role of authors

All authors had full access to all the data in the study and take responsibility for the integrity of the data and the accuracy of the data analysis. Study concept and design: JMR, HE, JS, and BC. Acquisition of data: JMR, HE, and CE. Analysis and interpretation of data: JMR, HE, JS, and BC. Drafting of the manuscript: JMR, JS, and BC. Critical revision of the manuscript for important intellectual content: JS, BC, and BW. Statistical analysis: JMR. Obtained funding: BC. Administrative, technical, and material support: BW and BC. Study supervision: JS and BC.

Grant support provided by the California Institute for Regenerative Medicine (CIRM) (RN1-00530-1 to BC), the National Institute of Health (R01 MH094589 to BC, GM085121 to JS), and Center for Molecular Medicine Cologne grant No D5 (to BW). Additional support was from Ellison Foundation for Medical Research and Center for Computational and Applied Transcriptomics (University of Copenhagen) (to JS). HE was supported by CIRM training award TG2-00157.

Literature Cited

Adachi K, Suemori H, Yasuda S, Nakatsuji N, Kawase E. Role of SOX2 in maintaining pluripotency of human embryonic stem cells. Genes to Cells. 2010; 15:455–470. [PubMed: 20384793]

Amrein H, Gorman M, Nöthiger R. The sex-determining gene tra-2 of Drosophila encodes a putative RNA binding protein. Cell. 1988; 55:1025–1035. [PubMed: 3144434]

Anderson ES, Lin C-H, Xiao X, Stoilov P, Burge CB, Black DL. The cardiotonic steroid digitoxin regulates alternative splicing through depletion of the splicing factors SRSF3 and TRA2B. RNA. 2012; 18:1041–1049. [PubMed: 22456266]

Angevine JB Jr, Sidman RL. Autoradiographic study of cell migration during histogenesis of cerebral cortex in the mouse. Nature. 1961; 192:766–768. [PubMed: 17533671]

Barbosa-Morais NL, Irimia M, Pan Q, Xiong HY, Gueroussov S, Lee LJ, Slobodeniuc V, Kutter C, Watt S, Çolak R, et al. The Evolutionary Landscape of Alternative Splicing in Vertebrate Species. Science. 2012; 338:1587–1593. [PubMed: 23258890]

Berry M, Rogers AW. The migration of neuroblasts in the developing cerebral cortex. J Anat. 1965; 99:691–709. [PubMed: 5325778]

Black DL. Mechanisms of Alternative Pre-Messenger Rna Splicing. Annual Review of Biochemistry. 2003; 72:291–336.

Blechingberg J, Holm IE, Nielsen AL. Characterization and expression analysis in the developing embryonic brain of the porcine FET family: FUS, EWS, and TAF15. Gene. 2012; 493:27–35. [PubMed: 22143032]

Boutz PL, Stoilov P, Li Q, Lin C-H, Chawla G, Ostrow K, Shiue L, Ares M Jr, Black DL. A post-transcriptional regulatory switch in polypyrimidine tract-binding proteins reprograms alternative splicing in developing neurons. Genes Dev. 2007; 21:1636–1652. [PubMed: 17606642]

Busch A, Hertel KJ. Evolution of SR protein and hnRNP splicing regulatory factors. Wiley Interdiscip Rev RNA. 2012; 3:1–12. [PubMed: 21898828]

Caffrey TM, Wade-Martins R. Functional MAPT haplotypes: Bridging the gap between genotype and neuropathology. Neurobiology of Disease. 2007; 27:1–10. [PubMed: 17555970]

Calarco JA, Zhen M, Blencowe BJ. Networking in a Global World: Establishing Functional Connections Between Neural Splicing Regulators and Their Target Transcripts. RNA. 2011; 17:775–791. [PubMed: 21415141]

Calif ice S, Baurain D, Hanikenne M, Motte P. A Single Ancient Origin for Prototypical Serine/Arginine-Rich Splicing Factors. Plant Physiol. 2012; 158:546–560. [PubMed: 22158759]

Castle JC, Zhang C, Shah JK, Kulkarni AV, Kalsotra A, Cooper TA, Johnson JM. Expression of 24,426 human alternative splicing events and predicted cis regulation in 48 tissues and cell lines. Nat Genet. 2008; 40:1416–1425. [PubMed: 18978788]

Caviness VS Jr, Takahashi T. Proliferative events in the cerebral ventricular zone. Brain Dev. 1995; 17:159–163. [PubMed: 7573753]

Cazalla D, Sanford JR, Cáceres JF. A rapid and efficient protocol to purify biologically active recombinant proteins from mammalian cells. Protein Expression and Purification. 2005; 42:54–58. [PubMed: 15878828]

Chen B, Schaevitz LR, McConnell SK. Fezl regulates the differentiation and axon targeting of layer 5 subcortical projection neurons in cerebral cortex. Proc Natl Acad Sci USA. 2005a; 102:17184–17189. [PubMed: 16284245]

Chen B, Wang SS, Hattox AM, Rayburn H, Nelson SB, McConnell SK. The Fezf2-Ctip2 genetic pathway regulates the fate choice of subcortical projection neurons in the developing cerebral cortex. Proc Natl Acad Sci USA. 2008; 105:11382–11387. [PubMed: 18678899]

Chen J-G, Rasin M-R, Kwan KY, Sestan N. Zfp312 is required for subcortical axonal projections and dendritic morphology of deep-layer pyramidal neurons of the cerebral cortex. Proc Natl Acad Sci USA. 2005b; 102:17792–17797. [PubMed: 16314561]

Chou S-J, Perez-Garcia CG, Kroll TT, O'Leary DDM. Lhx2 specifies regional fate in Emx1 lineage of telencephalic progenitors generating cerebral cortex. Nat Neurosci. 2009; 12:1381–1389. [PubMed: 19820705]

D'Souza I, Poorkaj P, Hong M, Nochlin D, Lee VM-Y, Bird TD, Schellenberg GD. Missense and silent tau gene mutations cause frontotemporal dementia with parkinsonism-chromosome 17 type, by affecting multiple alternative RNA splicing regulatory elements. PNAS. 1999; 96:5598–5603. [PubMed: 10318930]

Daoud R, Da Penha Berzaghi M, Siedler F, Hübener M, Stamm S. Activity-dependent regulation of alternative splicing patterns in the rat brain. European Journal of Neuroscience. 1999; 11:788–802. [PubMed: 10103073]

Dawson HN, Cantillana V, Chen L, Vitek MP. The Tau N279K Exon 10 Splicing Mutation Recapitulates Frontotemporal Dementia and Parkinsonism Linked to Chromosome 17 Tauopathy in a Mouse Model. J Neurosci. 2007; 27:9155–9168. [PubMed: 17715352]

DeFelipe J. Neocortical Neuronal Diversity: Chemical Heterogeneity Revealed by Colocalization Studies of Classic Neurotransmitters, Neuropeptides, Calcium-binding Proteins, and Cell Surface Molecules. Cereb Cortex. 1993; 3:273–289. [PubMed: 8104567]

Diez-Roux G, Banfi S, Sultan M, Geffers L, Anand S, Rozado D, Magen A, Canidio E, Pagani M, Peluso I, et al. A High-Resolution Anatomical Atlas of the Transcriptome in the Mouse Embryo. PLoS Biol. 2011; 9:e1000582. [PubMed: 21267068]

Ding D, Xu H, Liang Q, Xu L, Zhao Y, Wang Y. Over-expression of Sox2 in C3H10T1/2 cells inhibits osteoblast differentiation through Wnt and MAPK signalling pathways. International Orthopaedics (SICOT). 2012; 36:1087–1094.

Eckler MJ, McKenna WL, Taghvaei S, McConnell SK, Chen B. Fezf1 and Fezf2 are required for olfactory development and sensory neuron identity. J Comp Neurol. 2011; 519:1829–1846. [PubMed: 21452247]

Elliott DJ, Best A, Dalgliesh C, Ehrmann I, Grellscheid S. How does Tra2β protein regulate tissue-specific RNA splicing? Biochem Soc Trans. 2012; 40:784–788. [PubMed: 22817734]

Eom T, Zhang C, Wang H, Lay K, Fak J, Noebels JL, Darnell RB. NOVA-dependent regulation of cryptic NMD exons controls synaptic protein levels after seizure. Elife. 2013; 2:e00178. [PubMed: 23359859]

Garbes L, Heesen L, Hölker I, Bauer T, Schreml J, Zimmermann K, Thoenes M, Walter M, Dimos J, Peitz M, et al. VPA response in SMA is suppressed by the fatty acid translocase CD36. Hum Mol Genet. 2013; 22:398–407. [PubMed: 23077215]

Gorski JA, Talley T, Qiu M, Puelles L, Rubenstein JLR, Jones KR. Cortical excitatory neurons and glia, but not GABAergic neurons, are produced in the Emx1-expressing lineage. J Neurosci. 2002; 22:6309–6314. [PubMed: 12151506]

Götz M, Huttner WB. The cell biology of neurogenesis. Nat Rev Mol Cell Biol. 2005; 6:777–788. [PubMed: 16314867]

Graveley BR, Hertel KJ, Maniatis T. The role of U2AF35 and U2AF65 in enhancer-dependent splicing. RNA. 2001; 7:806–818. [PubMed: 11421359]

Graveley BR, Maniatis T. Arginine/serine-rich domains of SR proteins can function as activators of pre-mRNA splicing. Mol Cell. 1998; 1:765–771. [PubMed: 9660960]

Grellscheid S, Dalgliesh C, Storbeck M, Best A, Liu Y, Jakubik M, Mende Y, Ehrmann I, Curk T, Rossbach K, et al. Identification of Evolutionarily Conserved Exons as Regulated Targets for the Splicing Activator Tra2β in Development. PLoS Genet. 2011; 7:e1002390. [PubMed: 22194695]

Gulisano M, Broccoli V, Pardini C, Boncinelli E. Emx1 and Emx2 show different patterns of expression during proliferation and differentiation of the developing cerebral cortex in the mouse. Eur J Neurosci. 1996; 8:1037–1050. [PubMed: 8743751]

Han W, Kwan KY, Shim S, Lam MMS, Shin Y, Xu X, Zhu Y, Li M, Sestan N. TBR1 directly represses Fezf2 to control the laminar origin and development of the corticospinal tract. Proc Natl Acad Sci USA. 2011; 108:3041–3046. [PubMed: 21285371]

Hansen DV, Lui JH, Parker PRL, Kriegstein AR. Neurogenic radial glia in the outer subventricular zone of human neocortex. Nature. 2010; 464:554–561. [PubMed: 20154730]

Hartmann AM, Rujescu D, Giannakouros T, Nikolakaki E, Goedert M, Mandelkow E-M, Gao QS, Andreadis A, Stamm S. Regulation of Alternative Splicing of Human Tau Exon 10 by Phosphorylation of Splicing Factors. Molecular and Cellular Neuroscience. 2001; 18:80–90. [PubMed: 11461155]

Hayakawa H, Hayakawa M, Kume A, Tominaga S. Soluble ST2 Blocks Interleukin-33 Signaling in Allergic Airway Inflammation. J Biol Chem. 2007; 282:26369–26380. [PubMed: 17623648]

Hoch RV, Rubenstein JLR, Pleasure S. Genes and signaling events that establish regional patterning of the mammalian forebrain. Seminars in Cell & Developmental Biology. 2009; 20:378–386. [PubMed: 19560042]

Hofmann Y, Lorson CL, Stamm S, Androphy EJ, Wirth B. Htra2-β1 stimulates an exonic splicing enhancer and can restore full-length SMN expression to survival motor neuron 2 (SMN2). PNAS. 2000; 97:9618–9623. [PubMed: 10931943]

Hofmann Y, Wirth B. hnRNP-G promotes exon 7 inclusion of survival motor neuron (SMN) via direct interaction with Htra2-β1. Hum Mol Genet. 2002; 11:2037–2049. [PubMed: 12165565]

Hutton M, Lendon CL, Rizzu P, Baker M, Froelich S, Houlden H, Pickering-Brown S, Chakraverty S, Isaacs A, Grover A, et al. Association of missense and 5′-splice-site mutations in tau with the inherited dementia FTDP-17. Nature. 1998; 393:702–705. [PubMed: 9641683]

Hutton SR, Pevny LH. SOX2 expression levels distinguish between neural progenitor populations of the developing dorsal telencephalon. Developmental Biology. 2011; 352:40–47. [PubMed: 21256837]

Izquierdo JM, Valcárcel J. Fas-activated Serine/Threonine Kinase (FAST K) Synergizes with TIA-1/TIAR Proteins to Regulate Fas Alternative Splicing. J Biol Chem. 2007; 282:1539–1543. [PubMed: 17135269]

Jellinger KA. Interaction between pathogenic proteins in neurodegenerative disorders. Journal of Cellular and Molecular Medicine. 2012; 16:1166–1183. [PubMed: 22176890]

Joshi PS, Molyneaux BJ, Feng L, Xie X, Macklis JD, Gan L. Bhlhb5 Regulates the Postmitotic Acquisition of Area Identities in Layers II-V of the Developing Neocortex. Neuron. 2008; 60:258–272. [PubMed: 18957218]

Kohtz JD, Jamison SF, Will CL, Zuo P, Lührmann R, Garcia-Blanco MA, Manley JL. Protein-protein interactions and 5'-splice-site recognition in mammalian mRNA precursors. Nature. 1994; 368:119–124. [PubMed: 8139654]

Kwan KY, Šestan N, Anton ES. Transcriptional co-regulation of neuronal migration and laminar identity in the neocortex. Development. 2012; 139:1535–1546. [PubMed: 22492350]

Leone DP, Srinivasan K, Chen B, Alcamo E, McConnell SK. The determination of projection neuron identity in the developing cerebral cortex. Curr Opin Neurobiol. 2008; 18:28–35. [PubMed: 18508260]

Lewis BP, Green RE, Brenner SE. Evidence for the widespread coupling of alternative splicing and nonsense-mediated mRNA decay in humans. Proc Natl Acad Sci USA. 2003; 100:189–192. [PubMed: 12502788]

Li Q, Lee J-A, Black DL. Neuronal regulation of alternative pre-mRNA splicing. Nature Reviews Neuroscience. 2007; 8:819–831.

Long JC, Caceres JF. The SR protein family of splicing factors: master regulators of gene expression. Biochem J. 2009; 417:15. [PubMed: 19061484]

Lopez AJ. ALTERNATIVE SPLICING OF PRE-mRNA: Developmental Consequences and Mechanisms of Regulation. Annual Review of Genetics. 1998; 32:279–305.

McKenna WL, Betancourt J, Larkin KA, Abrams B, Guo C, Rubenstein JLR, Chen B. Tbr1 and Fezf2 Regulate Alternate Corticofugal Neuronal Identities during Neocortical Development. J Neurosci. 2011; 31:549–564. [PubMed: 21228164]

Mende Y, Jakubik M, Riessland M, Schoenen F, Rossbach K, Kleinridders A, Köhler C, Buch T, Wirth B. Deficiency of the splicing factor Sfrs10 results in early embryonic lethality in mice and has no impact on full-length SMN/Smn splicing. Hum Mol Genet. 2010; 19:2154–2167. [PubMed: 20190275]

Merkin J, Russell C, Chen P, Burge CB. Evolutionary dynamics of gene and isoform regulation in Mammalian tissues. Science. 2012; 338:1593–1599. [PubMed: 23258891]

Migliore M, Shepherd GM. Opinion: an integrated approach to classifying neuronal phenotypes. Nat Rev Neurosci. 2005; 6:810–818. [PubMed: 16276357]

Miyoshi G, Hjerling-Leffler J, Karayannis T, Sousa VH, Butt SJB, Battiste J, Johnson JE, Machold RP, Fishell G. Genetic Fate Mapping Reveals That the Caudal Ganglionic Eminence Produces a Large and Diverse Population of Superficial Cortical Interneurons. The Journal of Neuroscience. 2010; 30:1582–1594. [PubMed: 20130169]

Molyneaux BJ, Arlotta P, Hirata T, Hibi M, Macklis JD. Fezl is required for the birth and specification of corticospinal motor neurons. Neuron. 2005; 47:817–831. [PubMed: 16157277]

Molyneaux BJ, Arlotta P, Menezes JRL, Macklis JD. Neuronal subtype specification in the cerebral cortex. Nature Reviews Neuroscience. 2007; 8:427–437.

Ni JZ, Grate L, Donohue JP, Preston C, Nobida N, O'Brien G, Shiue L, Clark TA, Blume JE, Ares M. Ultraconserved elements are associated with homeostatic control of splicing regulators by alternative splicing and nonsense-mediated decay. Genes Dev. 2007; 21:708–718. [PubMed: 17369403]

Nicholson DW, Ali A, Thornberry NA, Vaillancourt JP, Ding CK, Gallant M, Gareau Y, Griffin PR, Labelle M, Lazebnik YA. Identification and inhibition of the ICE/CED-3 protease necessary for mammalian apoptosis. Nature. 1995; 376:37–43. [PubMed: 7596430]

O'Leary DD, Nakagawa Y. Patterning centers, regulatory genes and extrinsic mechanisms controlling arealization of the neocortex. Current Opinion in Neurobiology. 2002; 12:14–25. [PubMed: 11861160]

Owen N, Zhou H, Malygin AA, Sangha J, Smith LD, Muntoni F, Eperon IC. Design principles for bifunctional targeted oligonucleotide enhancers of splicing. Nucleic Acids Res. 2011; 39:7194–7208. [PubMed: 21602265]

Raj B, O'Hanlon D, Vessey JP, Pan Q, Ray D, Buckley NJ, Miller FD, Blencowe BJ. Cross-Regulation between an Alternative Splicing Activator and a Transcription Repressor Controls Neurogenesis. Molecular Cell. 2011; 43:843–850. [PubMed: 21884984]

Rallu M, Corbin JG, Fishell G. Parsing the prosencephalon. Nat Rev Neurosci. 2002; 3:943–951. [PubMed: 12461551]

Riedl SJ, Salvesen GS. The apoptosome: signalling platform of cell death. Nat Rev Mol Cell Biol. 2007; 8:405–413. [PubMed: 17377525]

Rubenstein JLR, Anderson S, Shi L, Miyashita-Lin E, Bulfone A, Hevner R. Genetic Control of Cortical Regionalization and Connectivity. Cereb Cortex. 1999; 9:524–532. [PubMed: 10498270]

Sanford JR, Ellis J, Cáceres JF. Multiple roles of arginine/serine-rich splicing factors in RNA processing. Biochem Soc Trans. 2005; 33:443–446. [PubMed: 15916537]

Shen H, Green MR. A pathway of sequential arginine-serine-rich domain-splicing signal interactions during mammalian spliceosome assembly. Mol Cell. 2004; 16:363–373. [PubMed: 15525510]

Shen H, Green MR. RS domain–splicing signal interactions in splicing of U12-type and U2-type introns. Nat Struct Mol Biol. 2007; 14:597–603. [PubMed: 17603499]

Shen H, Zheng X, Luecke S, Green MR. The U2AF35-related protein Urp contacts the 3′ splice site to promote U12-type intron splicing and the second step of U2-type intron splicing. Genes Dev. 2010; 24:2389–2394. [PubMed: 21041408]

Shepard PJ, Hertel KJ. The SR protein family. Genome Biol. 2009; 10:242. [PubMed: 19857271]

Staknis D, Reed R. SR proteins promote the first specific recognition of Pre-mRNA and are present together with the U1 small nuclear ribonucleoprotein particle in a general splicing enhancer complex. Mol Cell Biol. 1994; 14:7670–7682. [PubMed: 7935481]

Stoilov P, Daoud R, Nayler O, Stamm S. Human tra2-beta1 autoregulates its protein concentration by influencing alternative splicing of its pre-mRNA. Hum Mol Genet. 2004; 13:509–524. [PubMed: 14709600]

Taylor BJ, Villella A, Ryner LC, Baker BS, Hall JC. Behavioral and neurobiological implications of sex-determining factors in Drosophila. Developmental Genetics. 1994; 15:275–296. [PubMed: 8062459]

Vaccarino FM, Schwartz ML, Raballo R, Nilsen J, Rhee J, Zhou M, Doetschman T, Coffin JD, Wyland JJ, Hung Y-TE. Changes in cerebral cortex size are governed by fibroblast growth factor during embryogenesis. Nature Neuroscience. 1999; 2:485–485.

Visel A, Thaller C, Eichele G. GenePaint.org: an atlas of gene expression patterns in the mouse embryo. Nucleic Acids Res. 2004; 32:D552–D556. [PubMed: 14681479]

Volvert M-L, Rogister F, Moonen G, Malgrange B, Nguyen L. MicroRNAs tune cerebral cortical neurogenesis. Cell Death Differ. 2012; 19:1573–1581. [PubMed: 22858543]

Wakabayashi Y, Watanabe H, Inoue J, Takeda N, Sakata J, Mishima Y, Hitomi J, Yamamoto T, Utsuyama M, Niwa O, et al. Bcl11b is required for differentiation and survival of αβ T lymphocytes. Nat Immunol. 2003; 4:533–539. [PubMed: 12717433]

Wang ET, Sandberg R, Luo S, Khrebtukova I, Zhang L, Mayr C, Kingsmore SF, Schroth GP, Burge CB. Alternative isoform regulation in human tissue transcriptomes. Nature. 2008; 456:470–476. [PubMed: 18978772]

Wang J, Manley JL. Overexpression of the SR proteins ASF/SF2 and SC35 influences alternative splicing in vivo in diverse ways. RNA. 1995; 1:335–346. [PubMed: 7489505]

Wang J, Takagaki Y, Manley JL. Targeted disruption of an essential vertebrate gene: ASF/SF2 is required for cell viability. Genes Dev. 1996; 10:2588–2599. [PubMed: 8895660]

Wang Y, Wang J, Gao L, Lafyatis R, Stamm S, Andreadis A. Tau Exons 2 and 10, Which Are Misregulated in Neurodegenerative Diseases, Are Partly Regulated by Silencers Which Bind a SRp30c·SRp55 Complex That Either Recruits or Antagonizes htra2β1. J Biol Chem. 2005; 280:14230–14239. [PubMed: 15695522]

Watermann DO, Tang Y, zur Hausen A, Jäger M, Stamm S, Stickeler E. Splicing Factor Tra2-β1 Is Specifically Induced in Breast Cancer and Regulates Alternative Splicing of the CD44 Gene. Cancer Research. 2006; 66:4774–4780. [PubMed: 16651431]

Wilson AC, Peterson MG, Herr W. The HCF repeat is an unusual proteolytic cleavage signal. Genes Dev. 1995; 9:2445–2458. [PubMed: 7590226]

Wirth B, Garbes L, Riessland M. How genetic modifiers influence the phenotype of spinal muscular atrophy and suggest future therapeutic approaches. Curr Opin Genet Dev. 2013

Wu JY, Maniatis T. Specific interactions between proteins implicated in splice site selection and regulated alternative splicing. Cell. 1993; 75:1061–1070. [PubMed: 8261509]

Zahler AM, Neugebauer KM, Lane WS, Roth MB. Distinct functions of SR proteins in alternative pre-mRNA splicing. Science. 1993; 260:219–222. [PubMed: 8385799]

Zheng S, Gray EE, Chawla G, Porse BT, O'Dell TJ, Black DL. PSD-95 is post-transcriptionally repressed during early neural development by PTBP1 and PTBP2. Nat Neurosci. 2012; 15:381–388. [PubMed: 22246437]

Zhong X-Y, Wang P, Han J, Rosenfeld MG, Fu X-D. SR Proteins in Vertical Integration of Gene Expression from Transcription to RNA Processing to Translation. Molecular Cell. 2009; 35:1–10. [PubMed: 19595711]

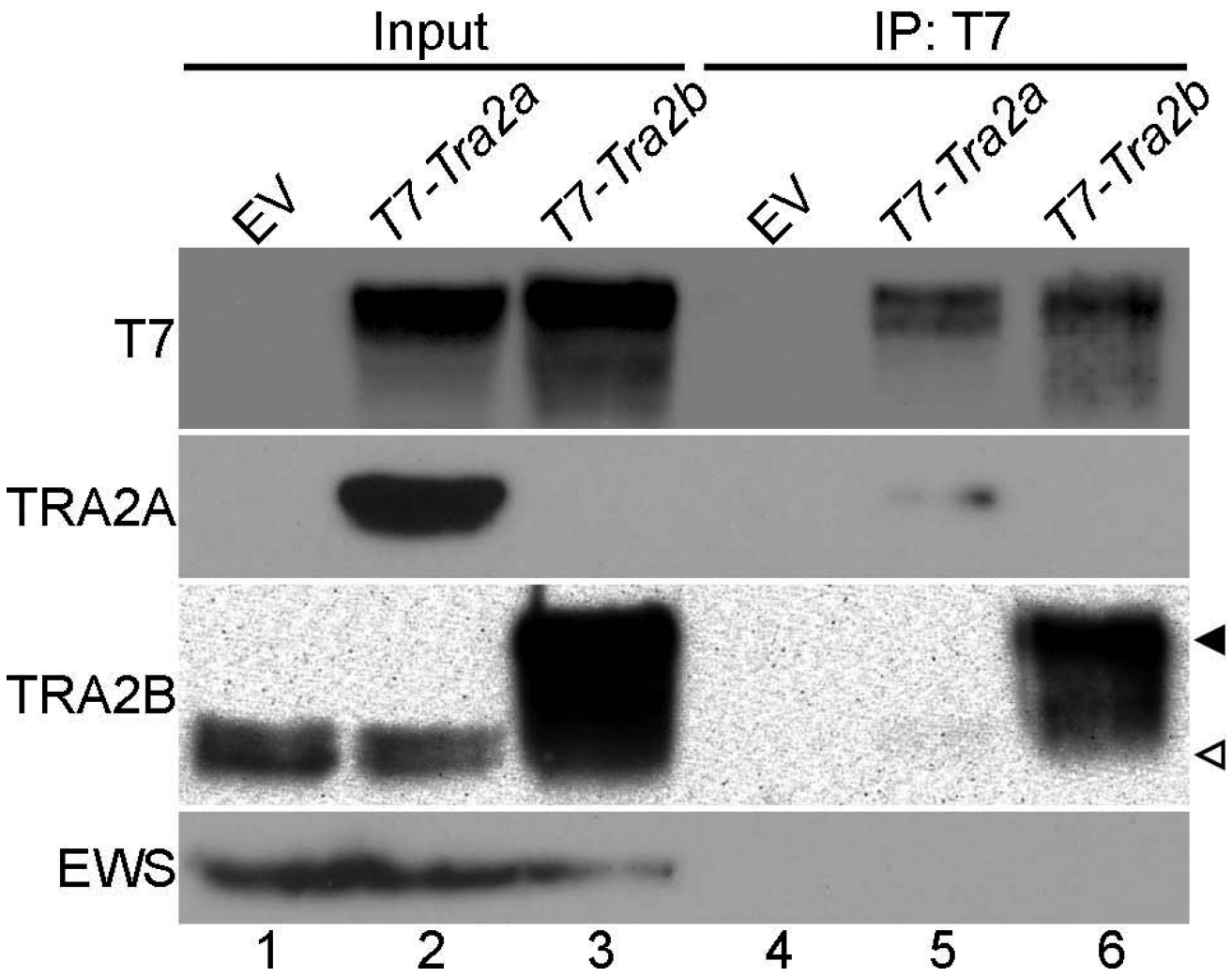

Figure 1.

TRA2B antibody does not react with TRA2A. Western blot analysis of cell lysates and immunoprecipitates (IPs) with anti-T7, anti-TRA2A, anti-TRA2B, and anti-EWS. Lanes 1-3, cell lysate from cells transfected with an empty vector (EV; lane 1), *T7-Tra2a* (lane 2), or *T7-Tra2b* (lane 3) expression vector. T7 is absent from lane 1, but strongly expressed in lanes 2 and 3. Anti-TRA2A detects exogenous T7-TRA2A in lane 2. Anti-TRA2B detects endogenous TRA2B in lanes 1-3, and exogenous T7-TRA2B in lane 3. EWS serves as a loading control, and is expressed at comparable levels in lanes 1-3. Lanes 4-6, T7 IP from cells transfected with EV (lane 4), *T7-Tra2a* (lane 5), or *T7-Tra2b* (lane 6). IP was selective for the T7 epitope, visible in lanes 5 and 6, and excluded non-tagged proteins. Anti-TRA2A detects T7-TRA2A in lane 5. Anti-TRA2B detects T7-TRA2B in lane 6, but not T7-TRA2A in lane 5. The black triangle indicates exogenous T7-TRA2B. The white triangle indicates endogenous TRA2B. No EWS is seen in lanes 4-6, confirming the specificity of the T7 IP.

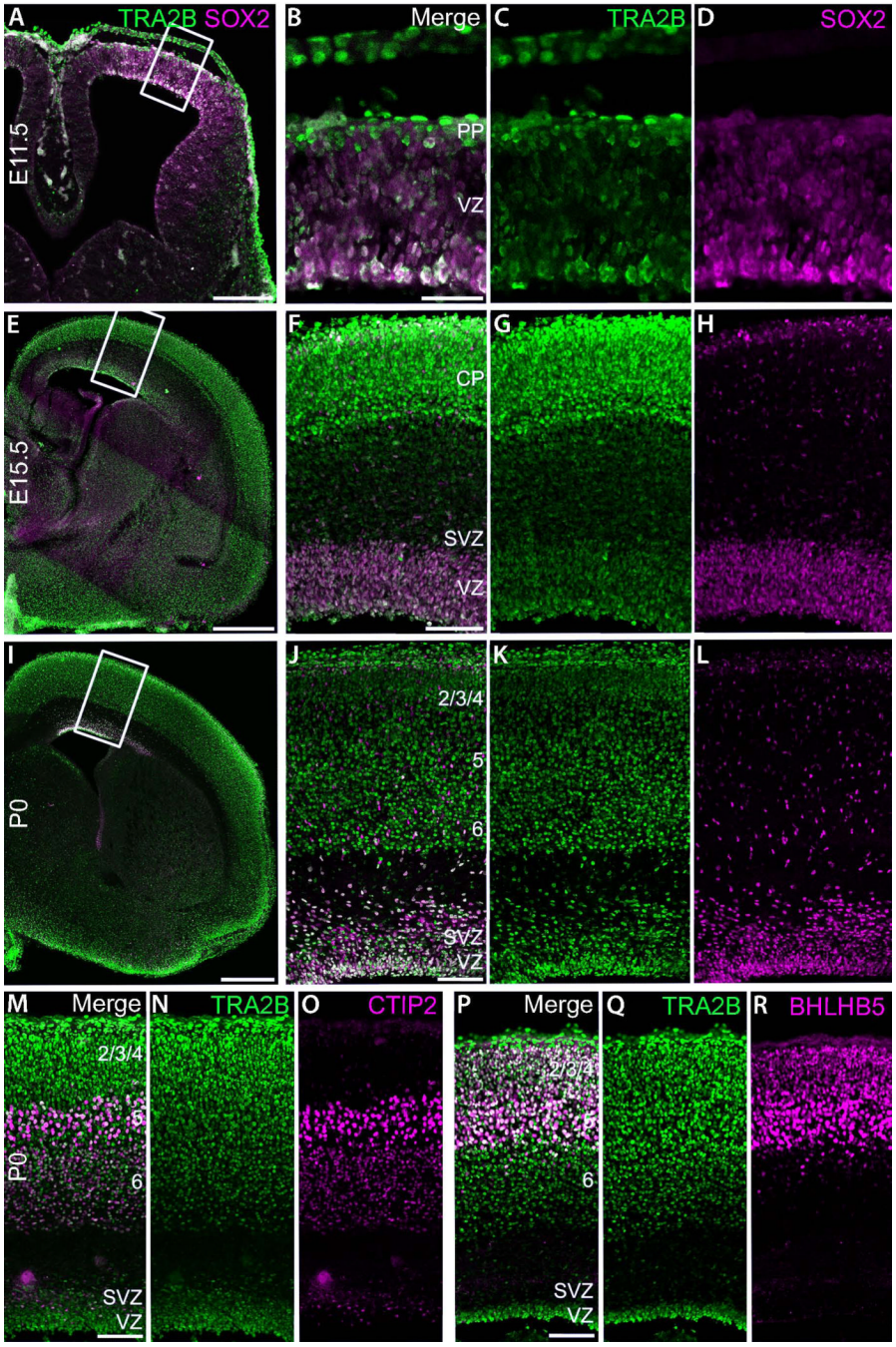

Figure 2.

TRA2B is expressed in neural progenitors and projection neurons during cortical development. A, E, I, Immunofluorescent coronal brain sections at E11.5 (A), E15.5 (E), and P0 (I) detected with anti-TRA2B (green) and anti-SOX2 (magenta) for identification of neural progenitors. B-D, F-H, J-L, Enlarged images of the developing cerebral cortex as indicated by boxed regions in A, E, and I. Multi-channel images (B, F, and J) are separated into individual channels to show TRA2B (C, G, and K) and SOX2 (D, H, and L) alone. M-R, Immunofluorescent P0 cerebral cortex detected with anti-TRA2B (M, P, green) and anti-CTIP2 (M, magenta) or anti-BHLHB5 (P, magenta), and separated into individual channels for TRA2B (N, Q), CTIP2 (O), and BHLHB5 (R). CP, cortical plate; PP, pre-plate; SVZ,

sub-ventricular zone; VZ, ventricular zone. Scale bars: A, 250 μm; B-D, 50 μm; E, 500 μm; F-H, 250 μm; I, 500 μm; J-L, M-R, 250 μm.

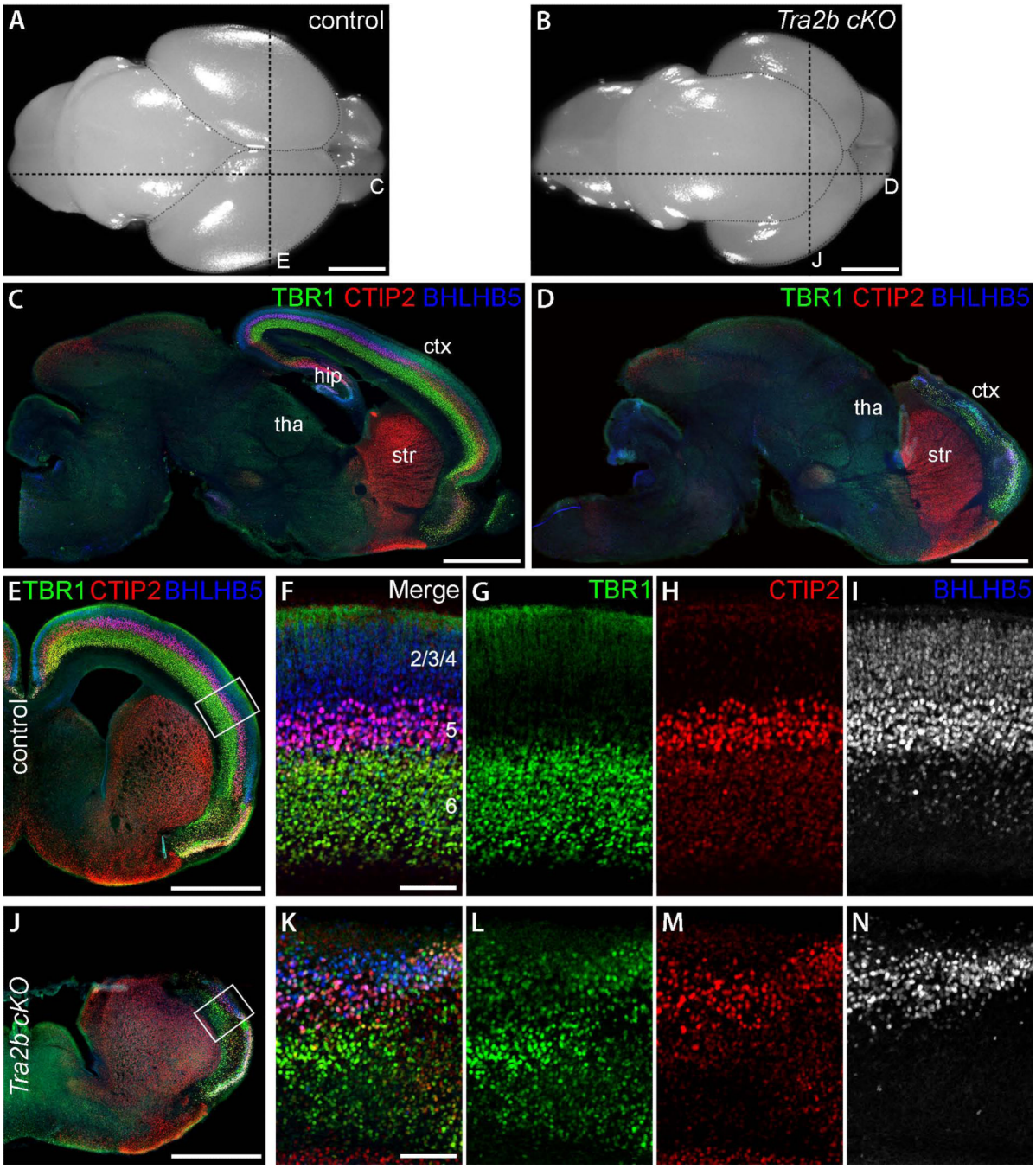

Figure 3.

Tra2b cKO mice have smaller, disorganized cortices. Comparisons were made between P0 control (A, C, E-I) and *cKO* (B, D, J-N) littermates. A, B, Whole mount brains, with cortex outlined to identify borders and dotted lines indicating sectioning planes for accompanying panels. C-N, Immunofluorescent brain sections detected with anti-TBR1 (green), anti-CTIP2 (red), and anti-BHLHB5 (blue) to identify cortical projection neuron populations. Sagittal sections (C, D) demonstrate the absence of the caudal cortex (ctx) and hippocampus (hip) in the *cKO* (D). Coronal sections (E, J) demonstrate the absence of the medial cortex in the *cKO* (J). Boxed areas in E and J are enlarged in F and K to show the cortical neuron layering

and are separated into individual channels with TBR1 (G, L), CTIP2 (H, M), or BHLHB5 (I, N) staining. str, striatum; tha, thalamus. Scale bars: A-E, J, 1 mm; F-I, K-N, 100 μm.

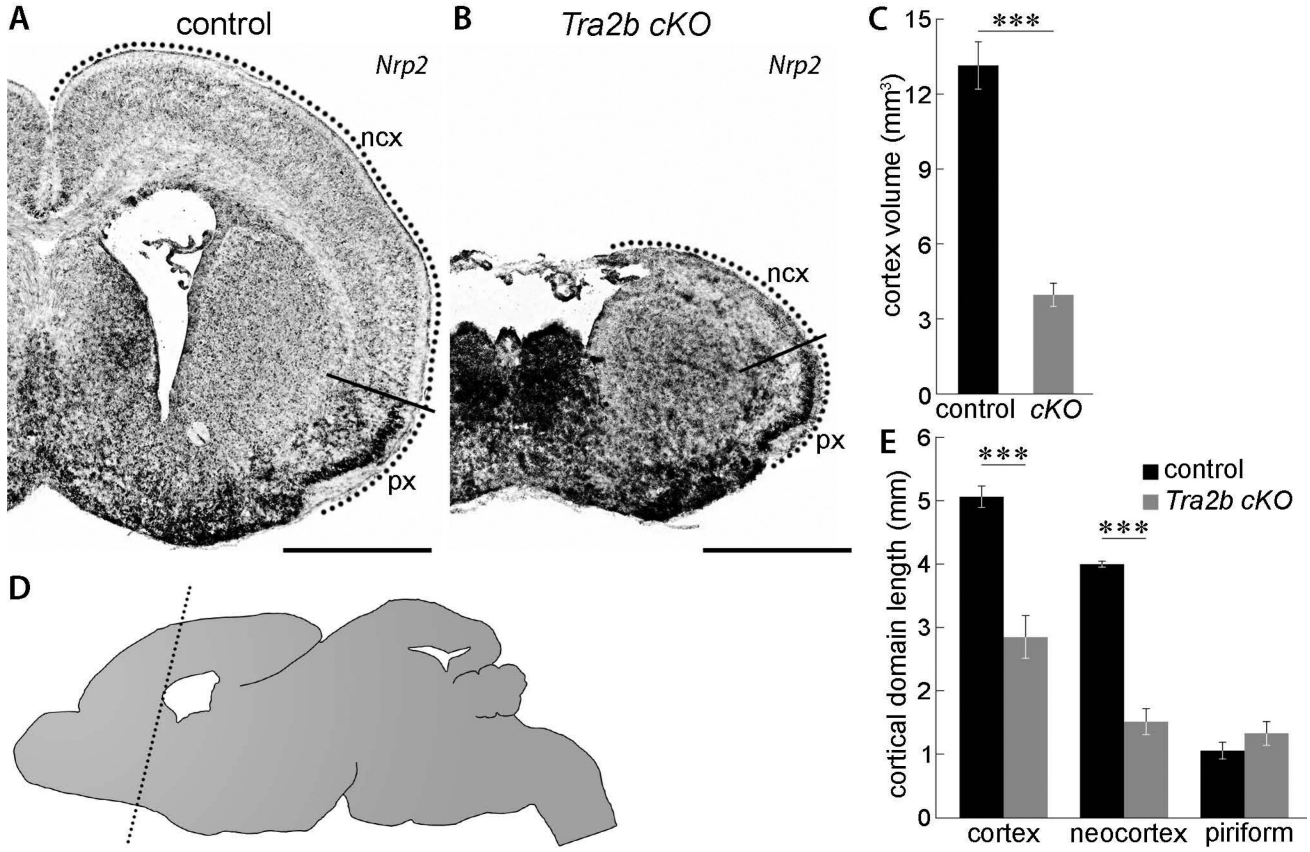

Figure 4.

Tra2b cKO mice have a smaller neocortex but the piriform cortex is not apparently affected. A, B, Coronal sections of control (A) and *cKO* (B) P0 brains, probed for *Nrp2* by *in situ* hybridization. *Nrp2* was highly expressed in the piriform cortex (px) and expressed at a lower level in the neocortex (ncx). Solid lines highlight the border between the piriform cortex and neocortex. Dotted lines indicate the surface of the cortex, measured to determine the length of cortical domains (quantified in D). C, Total cortex volume was significantly reduced in the *cKO*. The volume of control and *Tra2b cKO* cortecies were 13.1 ± 1.0 mm^3 and 4.0 ± 0.5 mm^3 respectively. D, Schematic representation of the anterior-posterior position of the coronal sections used for measuring the length of cortical domains. The sectioning plane is indicated by a dotted line. E, Quantification of cortical domain lengths. Cortex length was significantly reduced from 5.0 ± 0.2 mm to 2.8 ± 0.3 mm in the *cKO*. The length of the neocortex was also reduced from 4.0 ± 0.1 mm to 1.5 ± 0.2 mm. The piriform cortex length is not significantly different between 1.1 ± 0.1 mm in the control to 1.3 ± 0.2 mm in the *cKO*. Data are mean ± SD. n=3 brains analyzed per genotype; ****P<0.005*. Scale bars: A, B, 1 mm.

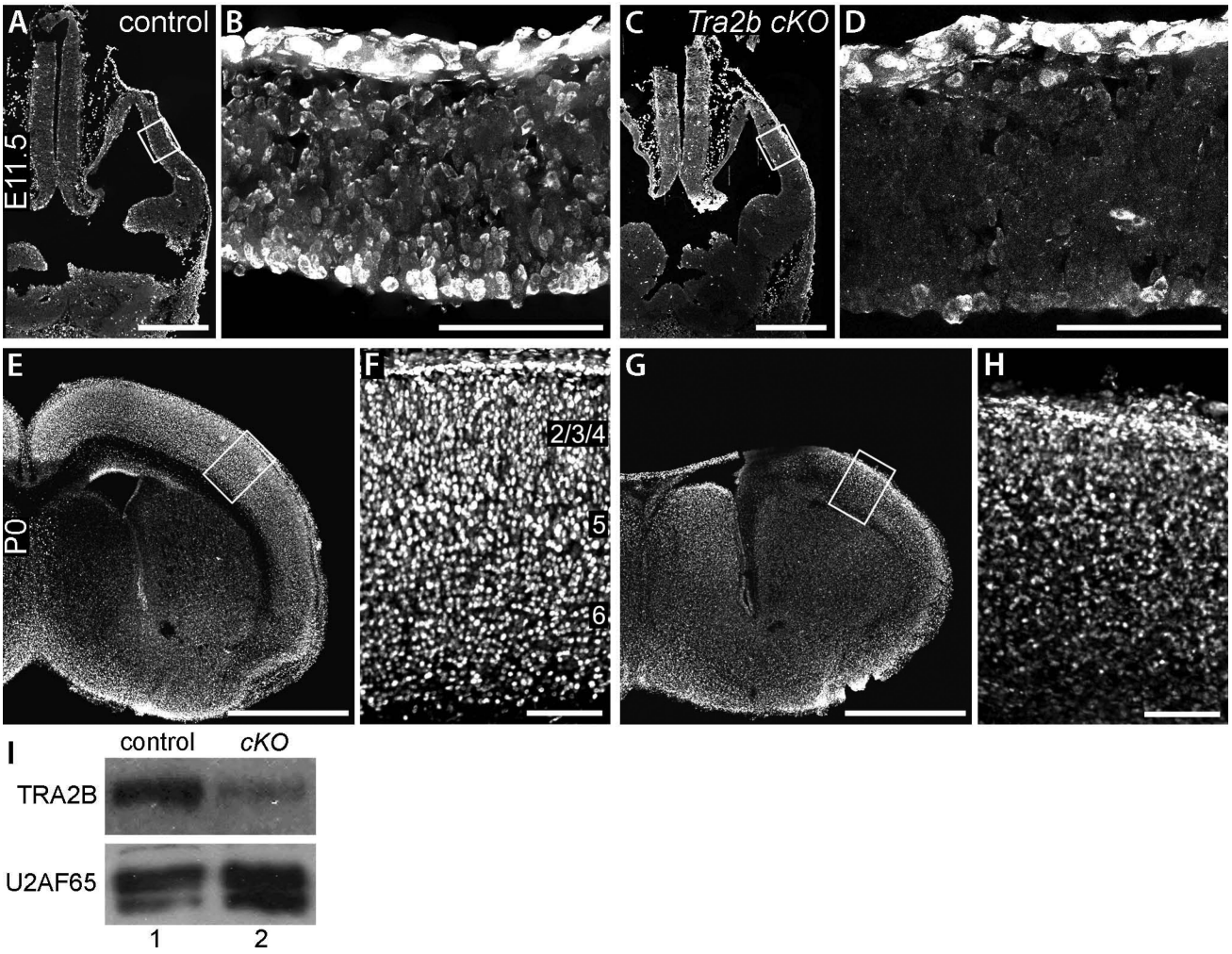

Figure 5.

TRA2B is reduced in the *Tra2b cKO* cerebral cortex. A-H, Coronal brain sections, immunostained for TRA2B. E11.5 control (A, B) and *Tra2b cKO* (C, D), and P0 control (E, F) and *Tra2b cKO* (G, H). Boxed areas from A, C, E, and G are enlarged in B, D, F, and H respectively. I, Western blot analysis of P0 cortical protein extracts. TRA2B is reduced in the Tra2b cKO sample (lane 2) compared to the control (lane 1). U2AF65 serves as the loading control. Scale bars: A, C, 500 μm; B, D, F, H, 100 μm; E, G, 1 mm.

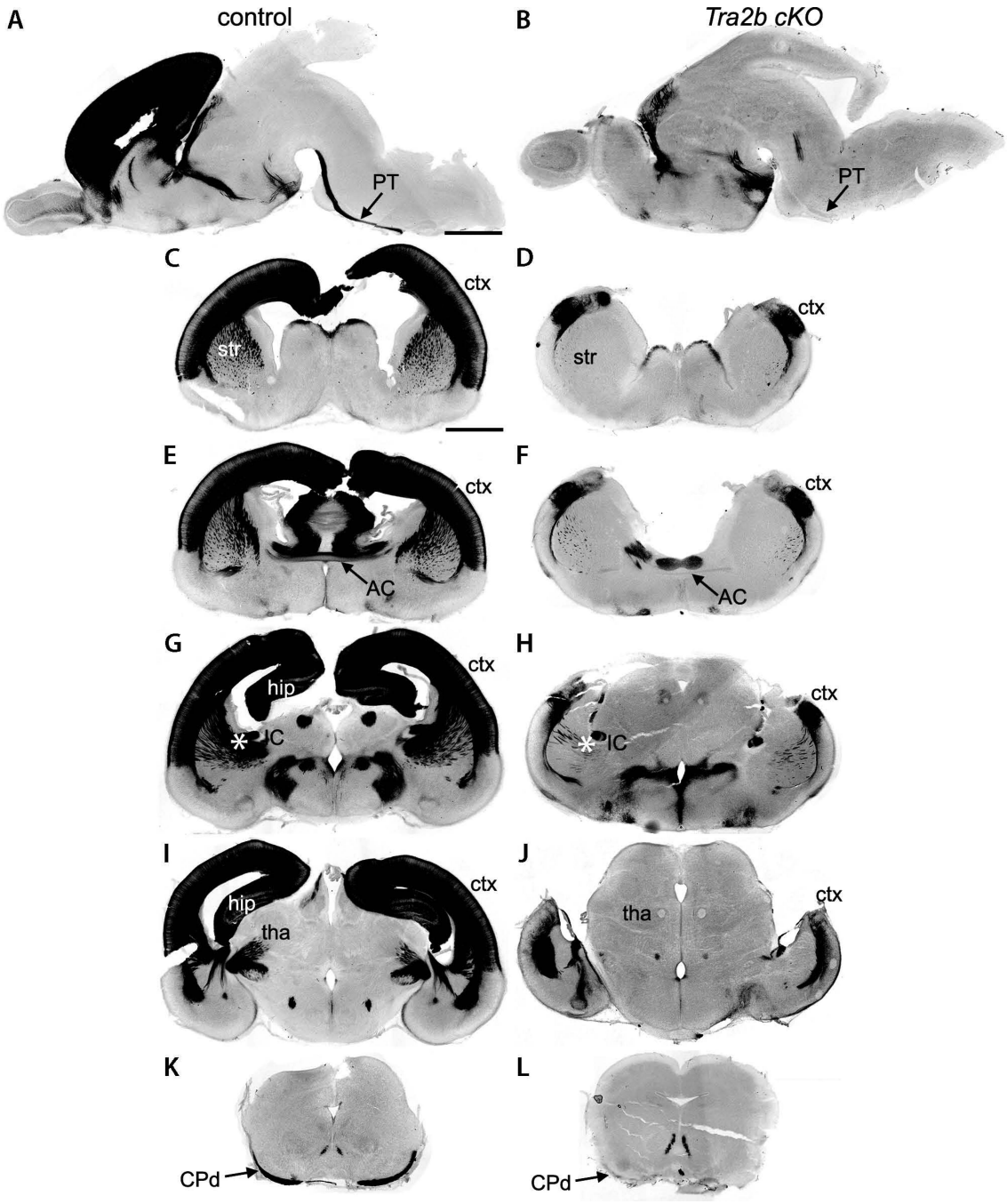

Figure 6.

Severe reduction of subcortical axons in *Tra2b cKO* assayed using the *Fezf2-PLAP* allele. P0 brains from *Emx1-cre; Tra2b*$^{fl/+}$*; Fezf2*$^{PLAP/+}$ (control) and *Emx1-cre; Tra2b*$^{fl/fl}$*; Fezf2*$^{PLAP/+}$ cKO mice are shown, enzymatically stained for PLAP. A, B, Sagittal sections from control (A) and *cKO* (B) brains. C-L, Coronal sections from control (C, E, G, I, K) and *cKO* (D, F, H, J, L). Arrows point to the anterior commissure, AC (E, F); cerebral peduncle, CPd (K, L); and pyramidal tract, PT (A, B). Asterisks indicate the internal capsule, IC (G, H). ctx, cerebral cortex; hip, hippocampus; str, striatum; tha, thalamus. Scale bars: 1 mm.

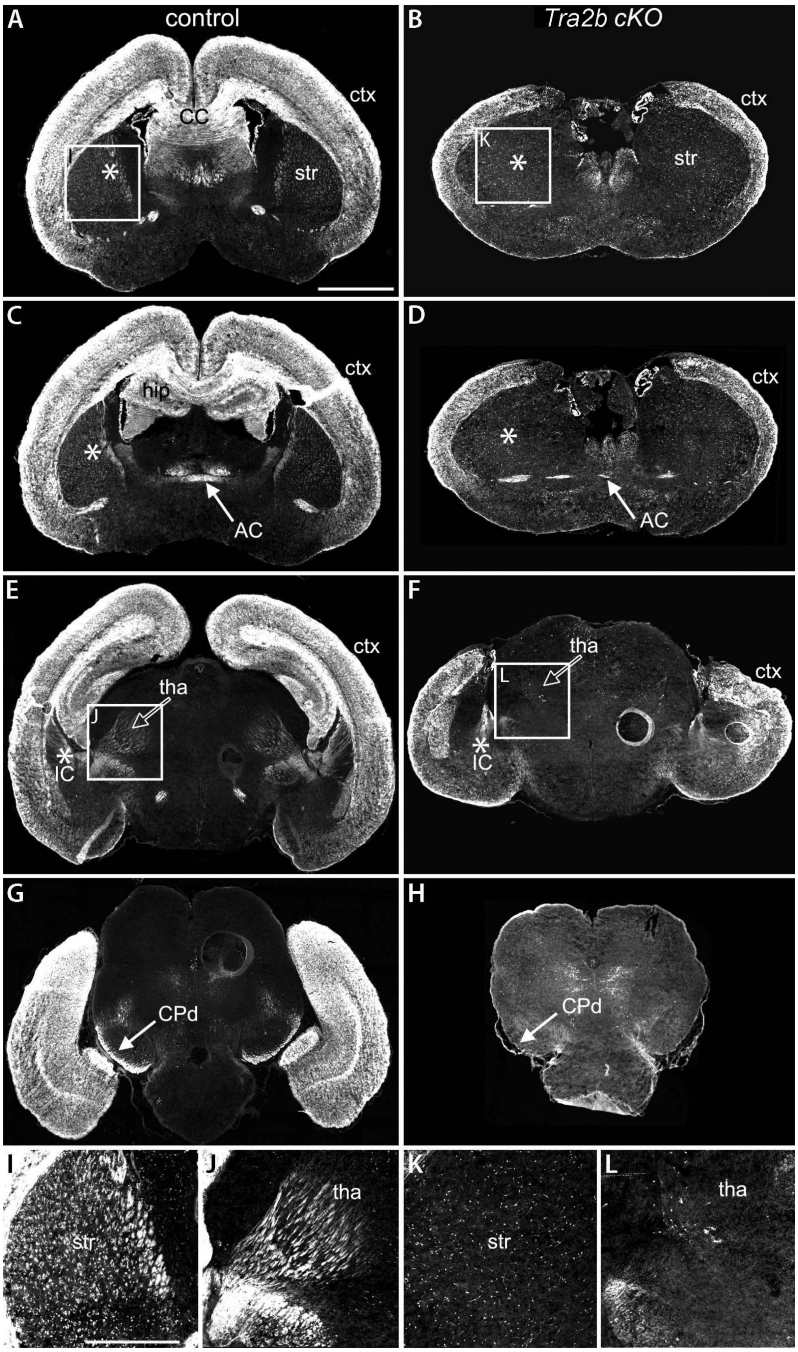

Figure 7.

Severe reduction of cortical axons assayed using the *RCE-GFP* CRE reporter allele. P0 brains from *Emx1-cre; Tra2b*$^{fl/+}$*; RCE-GFP* (control) and *Emx1-cre; Tra2b*$^{fl/fl}$*; RCE-GFP* cKO mice are shown. A-H, Coronal brains sections from control (A, C, E, G) and *cKO* (B, D, F, H) brains were stained with anti-GFP antibody. I-L, Enlarged images of boxed regions in A, B, E, and F, respectively. Asterisks indicate the internal capsule, IC (A-F). Filled arrows point to the anterior commissure, AC (C, D) and cerebral peduncle, CPd (G, H). Empty arrows point to the thalamus, tha (E, F). CC, corpus collosum; ctx, cerebral cortex; hip, hippocampus; str, striatum; tha, thalamus. Scale bars: A-H, 1 mm; I-L, 500 μm.

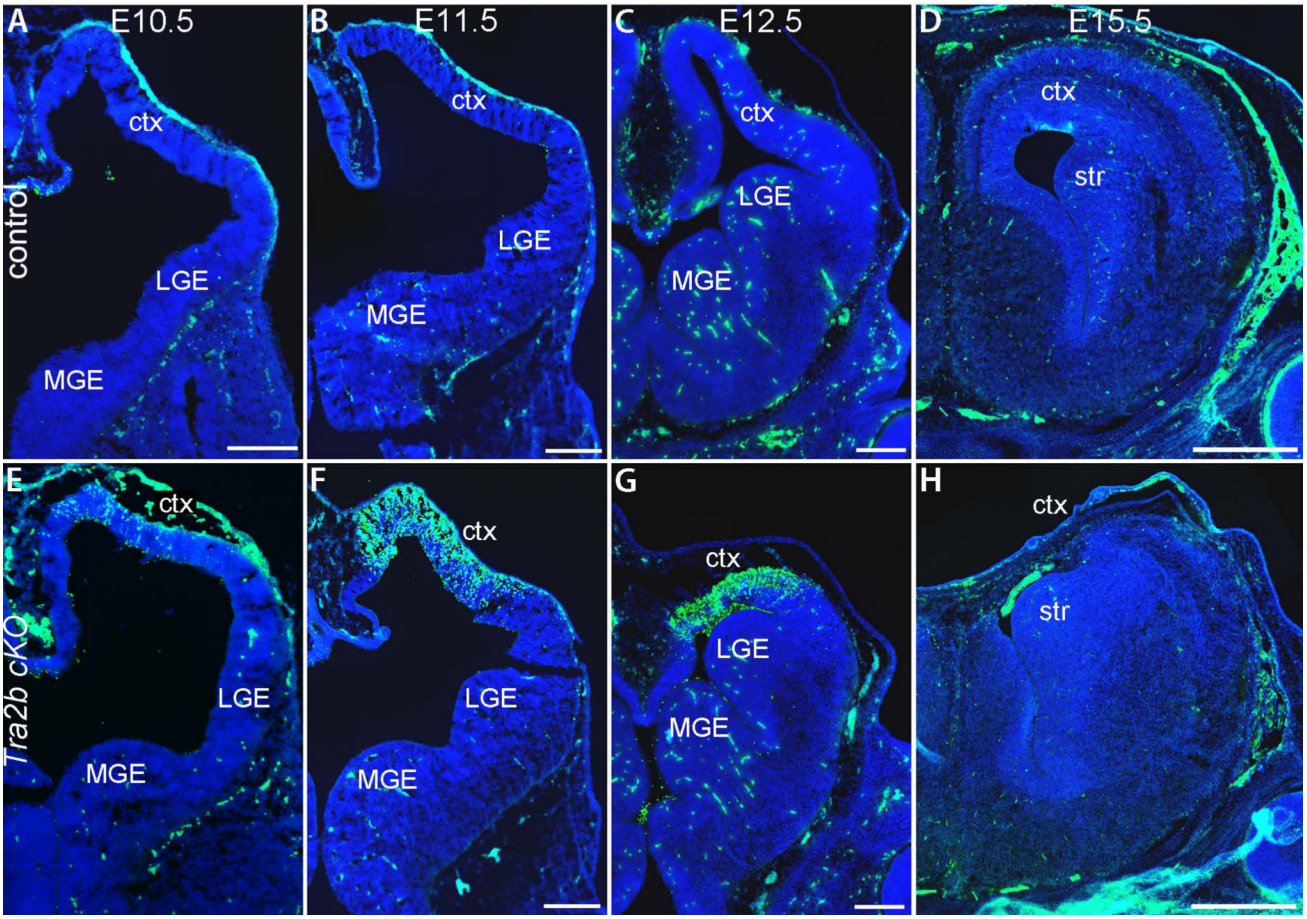

Figure 8.

Increased apoptosis in *Tra2b cKO* during neurogenesis. A-H, Immunofluorescent coronal brain sections detected with anti-cleaved Caspase-3 antibody (CC3, green). Blue represents DRAQ5 nuclear stain. Control (A-D) and *Tra2b cKO* (E-H) brains are compared at E10.5 (A, E), E11.5 (B, F), E12.5 (C, G), and E15.5 (D, H). ctx, cerebral cortex; LGE, lateral ganglionic eminence; MGE, medial ganglionic eminence; str, striatum. Scale bars: A-C, E-G, 200 μm; D, H, 500 μm.

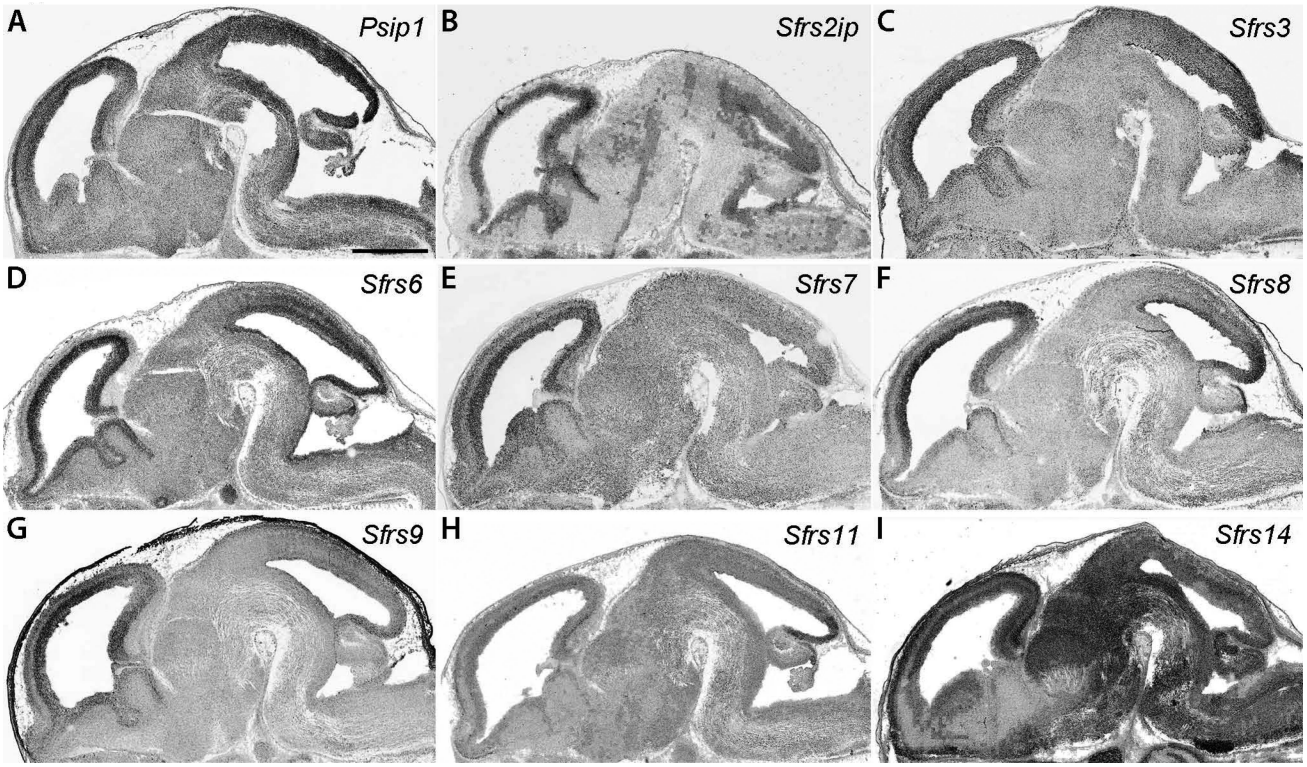

Figure 9.

In situ hybridization analysis of SR and SR-related protein family members. A-I, Sagittal sections from E14.5 wild-type mice probed for *Psip1* (A), *Sfrs2ip* (B), *Sfrs3* (C), *Sfrs6* (D), *Sfrs7* (E), *Sfrs8* (F), and *Sfrs9* (G), *Sfrs11* (H), *Sfrs14* (I). Panels A, C, E, F and G were obtained from GenePaint (www.genepaint.org) and panels B, D, H and I were obtained from Eurexpress (www.eurexpress.org). Scale bar: 1 mm.

Table 1

List of primary antibodies used in this study.

Antibody (clone)	Host	Source (Catalog No.)	Dilution	Immunogen
BHLHB5	goat (P)	Santa Cruz Biotechnology, Santa Cruz, CA (sc-6045)	1:100	KLH-conjugated peptide: ERGLHLGAAAASEDDLFL
cleaved Caspase-3	rabbit (P)	Cell Signaling Technology, Danvers, MA (9661)	1:100	KLH-conjugated peptide: CRGTELDCGIETD
CTIP2 (25B6)	rat (M)	Abcam, Cambridge, MA (ab18465)	1:1000	GST-conjugated peptide: residues 1-173 of CTIP2
EWS (C-9)	mouse (M)	Santa Cruz Biotechnology (sc-48404)	1:500	KLH-conjugated peptide: residues 2-43 of EWS
GFP	chicken (P)	Aves Labs, Tigard, OR (GFP-1020)	1:500	Purified recombinant EGFP
SOX2	goat (P)	Santa Cruz Biotechnology (sc-17320)	1:500	KLH-conjugated peptide: YLPGAEVPEPAAPSRLH
T7	rabbit (P)	Bethyl Laboratories, Montgomery, TX (A190)	1:5000	KLH-conjugated peptide: MASMTGGQQMG
T7-agarose	mouse (M)	Novagen, EMD Milipore, Billerica, MA (69026-3)	1:35	T7 epitope: MASMTGGQQMG
TBR1	rabbit (P)	Abcam (ab31940)	1:500	KLH-conjugated peptide: TDNFPDSKDSPGDVQRSK
TRA2A	mouse (P)	Sigma-Aldrich, St. Louis, MO (SAB1400517)	1:1000	GST-conjugated peptide: residues 1-282 of TRA2A
TRA2B	rabbit (P)	Dr. Brunhilde Wirth	1:8000	KLH-conjugated peptide: MSDSGEQNYGERESR
U2AF65 (MC3)	mouse (M)	Santa Cruz Biotechnology (sc-53942)	1:1000	Purified recombinant U2AF65

(P), polyclonal; (M), monoclonal

Table 2

Abbreviations for anatomical structures used in text and figures.

AC	anterior commissure
CC	corpus collossum
CP	cortical plate
CPd	cerebral peduncle
ctx	cerebral cortex
hip	hippocampus
IC	internal capsule
LGE	lateral ganglionic eminence
MGE	medial ganglionic eminence
ncx	neocortex
PP	pre-plate
PT	pyramidal tract
px	piriform cortex
str	striatum
SVZ	sub-ventricular zone
tha	thalamus
VZ	ventricular zone